Appl. Comput. Harmon. Anal. 26 (2009) 249–269

Contents lists available at ScienceDirect

Applied and Computational Harmonic Analysis

www.elsevier.com/locate/acha

Orthogonal Helmholtz decomposition in arbitrary dimension using divergence-free and curl-free wavelets

Erwan Deriaz [a,*], Valérie Perrier [b]

[a] Institute of Mathematics, Polish Academy of Sciences, ul. Śniadeckich 8, 00-956 Warszawa, Poland
[b] Laboratoire Jean Kuntzmann, Université de Grenoble and CNRS, BP 53, 38 041 Grenoble cedex 9, France

ARTICLE INFO

Article history:
Received 23 April 2007
Revised 2 March 2008
Accepted 5 June 2008
Available online 11 June 2008
Communicated by
Pierre G. Lemarié-Rieusset

ABSTRACT

We present tensor-product divergence-free and curl-free wavelets, and define associated projectors. These projectors enable the construction of an iterative algorithm to compute the Helmholtz decomposition of any vector field, in wavelet domain. This decomposition is localized in space, in contrast to the Helmholtz decomposition calculated by Fourier transform. Then we prove the convergence of the algorithm in dimension two for any kind of wavelets, and in larger dimension for the particular case of Shannon wavelets. We also present a modification of the algorithm by using quasi-isotropic divergence-free and curl-free wavelets. Finally, numerical tests show the validity of this approach for a large class of wavelets.

0. Introduction

In many physical problems, like the simulation of incompressible fluids (Stokes problem, Navier–Stokes equations [2,23]), or in electromagnetism (Maxwell's equations [22]), the solution has to fulfill a divergence-free condition. The implementation of relevant numerical schemes often requires the orthogonal projection of the solution, onto the set of divergence-free vector valued functions.

The Helmholtz decomposition [2,14] consists in splitting a vector field $\mathbf{u} \in (L^2(\mathbb{R}^n))^n$, into its divergence-free component $\mathbf{u}_{\text{div}}$ and its curl-free component $\mathbf{u}_{\text{curl}}$. More precisely, there exist a stream-function ψ (scalar in the 2D case and divergence-free vector valued for $n \geqslant 3$) and a potential-function p such that:

$$\mathbf{u} = \mathbf{u}_{\text{div}} + \mathbf{u}_{\text{curl}} \tag{0.1}$$

with

$$\mathbf{u}_{\text{div}} = \operatorname{curl} \psi \quad (\operatorname{div} \mathbf{u}_{\text{div}} = 0) \quad \text{and} \quad \mathbf{u}_{\text{curl}} = \nabla p \quad (\operatorname{curl} \mathbf{u}_{\text{curl}} = 0).$$

Moreover, the functions $\operatorname{curl} \psi$ and ∇p are orthogonal in $(L^2(\mathbb{R}^n))^n$. The stream-function ψ and the potential-function p are unique, up to an additive constant.

This decomposition arises from the orthogonal direct sum of the two spaces $\mathbf{H}_{\text{div}\,0}(\mathbb{R}^n)$, the space of divergence-free vector functions, and $\mathbf{H}_{\text{curl}\,0}(\mathbb{R}^n)$, the space of curl-free vector functions. In short:

$$\left(L^2(\mathbb{R}^n)\right)^n = \mathbf{H}_{\text{div}\,0}\left(\mathbb{R}^n\right) \oplus^{\perp} \mathbf{H}_{\text{curl}\,0}\left(\mathbb{R}^n\right).$$

* Corresponding author.
E-mail addresses: e.deriaz@impan.gov.pl (E. Deriaz), valerie.perrier@imag.fr (V. Perrier).

1063-5203/$ – see front matter
doi:10.1016/j.acha.2008.06.001

This decomposition is straightforward in $(L^2(\mathbb{R}^n))^n$ thanks to the Leray projector (the orthogonal projector from $(L^2(\mathbb{R}^n))^n$ onto $\mathbf{H}_{\mathrm{div}\,0}(\mathbb{R}^n)$) which can be explicitly described in Fourier domain. The Helmholtz decomposition (0.1) also exists for more general open sets Ω [2,14].

The objective of the present paper is to propose an efficient way to compute the orthogonal Helmholtz decomposition of any vector field, in wavelet domain. Since wavelet bases are localized both in physical and Fourier spaces [15], the advantages of such a decomposition, in contrast with the one based on the Fourier transform, are its localization in physical space and its availability on the whole domain $\mathbb{R}^n$, as well as on bounded domains. Moreover, an accurate wavelet Helmholtz decomposition would be provided by a small number of degrees of freedom, thanks to nonlinear approximation properties of wavelet bases [4]. This last property will be of great interest, for instance in direct numerical simulations (DNS) of turbulence [11].

In this context compactly supported divergence-free wavelets have been originally designed by Lemarié-Rieusset in the whole space $\mathbb{R}^n$ [16], as well as in the cube $[0,1]^n$ [17]. These functions have been investigated and supplement by curl-free wavelets for the decomposition of $\mathbf{H}_{\mathrm{div}\,0}(\mathbb{R}^n)$ and $\mathbf{H}_{\mathrm{curl}\,0}(\mathbb{R}^n)$ by Urban in [1,26]. Since divergence-free and curl-free wavelets are biorthogonal bases (and not orthogonal, see [18], unless having an infinite support [24]), the associated projectors do not provide directly the Helmholtz decomposition of a vector field. Therefore we have originally proposed an iterative algorithm in [8], of which we have proved the convergence in dimensions 2 and 3, using Shannon wavelets [9]. In order to achieve the convergence of the algorithm in any dimension, we propose in this article a new formulation for the divergence-free and curl-free wavelets, in dimensions larger than 4. This re-formulation will be based on the expression of the Leray projector in wavelet domain, which we want to be analogous to its expression in Fourier domain: this analogy is one of the key-points that allow to prove the convergence of the algorithm in dimension larger than three for Shannon wavelets, and to construct quasi-isotropic divergence-free wavelets. We generalize the proof of convergence in the bivariate case for all kind of wavelets, under some hypothesis on the Fourier transform of the wavelets, used to build the divergence-free and curl-free bases.

The article is organized as follows: in Section 1 we review the basic facts for the construction of divergence-free and curl-free wavelets, with an efficient way to compute the corresponding coefficients. Then we describe our construction for anisotropic wavelet bases of $\mathbf{H}_{\mathrm{div}\,0}(\mathbb{R}^n)$ and $\mathbf{H}_{\mathrm{curl}\,0}(\mathbb{R}^n)$ in dimension larger than 4, and describe their associated projectors. Section 2 is devoted to the description of iterative procedures to compute in practice the wavelet Helmholtz decomposition of any vector field, and to the study of the algorithm convergence: we first prove the convergence of the algorithm in the bivariate case, for any choice of wavelets. In general dimension, we prove the convergence of the method in the particular case of Shannon wavelets. In Section 3, we modify the expression of our wavelets, in order to propose quasi-isotropic divergence-free and curl-free wavelets, for which we prove the convergence of the method. Finally, we present in Section 4 numerical tests, to observe the convergence of the wavelet Helmholtz decomposition algorithm on 2D and 3D vector fields: In particular, we will study the convergence rate according to the number of vanishing moments of the wavelets; we will also see that pure isotropic wavelets do not lead to the convergence of our method, contrary to quasi-isotropic or pure anisotropic wavelets.

1. Divergence-free and curl-free wavelets

1.1. Lemarié's fundamental theorem on wavelet derivative

Compactly supported divergence-free wavelets have been constructed by Lemarié-Rieusset in 1992 [16]. These functions have been used by Urban in the numerical simulation of the Stokes problem [25]; moreover, curl-free wavelets have been constructed and analyzed in [26]. These constructions are both based on the existence of *biorthogonal wavelet bases* (see [3,19]) linked by differentiation. In particular, we will use the following result from [16]:

Proposition 1.1. *Let (V_j^1) be a multi-resolution analysis (MRA) of $L^2(\mathbb{R})$, with associated wavelet ψ_1 and scaling function φ_1. Then there exists a MRA (V_j^0), with associated wavelet ψ_0 and scaling function φ_0, satisfying:*

$$\psi_1'(x) = 4\psi_0(x) \quad \textit{and} \quad \varphi_1'(x) = \varphi_0(x) - \varphi_0(x-1). \tag{1.1}$$

Similar relations hold for the dual functions (φ_1^*, ψ_1^*) and (φ_0^*, ψ_0^*) of the primal ones (φ_1, ψ_1) and (φ_0, ψ_0):

$$\psi_0^{*'}(x) = -4\psi_1^*(x) \quad \textit{and} \quad \varphi_0^{*'}(x) = \varphi_1^*(x+1) - \varphi_1^*(x).$$

By this theorem, we have at hand two Riesz bases of $L^2(\mathbb{R})$:

$$\big(\psi_{1,j,k}(x) = 2^{j/2}\psi_1\big(2^j x - k\big)\big)_{j,k\in\mathbb{Z}} \quad \text{and} \quad (\psi_{0,j,k})_{j,k\in\mathbb{Z}}$$

linked by differentiation. Hence a function decomposed into the first basis $\psi_{1,j,k}$ with coefficients $(d_{j,k})$, has for derivative the function with coefficients $(2^{j+2}d_{j,k})$ into the second basis $\psi_{0,j,k}$. Conversely an indefinite integral of function of coefficients $(d_{j,k})$ into the second basis $\psi_{0,j,k}$, has for coefficients $(2^{-j-2}d_{j,k})$ into the first one.

Contrarily to the wavelets proposed in Lemarié-Rieusset's and Urban's works, we will prefer to use *anisotropic* divergence-free and curl-free wavelet bases, which means tensor-products of one-dimensional wavelet bases. Indeed in the 2D and 3D anisotropic cases, we have proposed in [6,8], Fast Wavelet Transforms which do not need the practical construction of the dual functions of divergence-free and curl-free wavelets (contrary to [15]). Our transforms are based on the construction of particular complement spaces, and we will detail the principles in the next section, in the bivariate case, for sake of clarity.

1.2. Bivariate anisotropic divergence-free and curl-free wavelets

1.2.1. Bivariate divergence-free wavelets

Anisotropic divergence-free wavelets in two dimensions are constructed by taking the curl of wavelets of the tensor-product MRA $(V_j^1 \otimes V_j^1)$:

$$\Psi_{\mathbf{j},\mathbf{k}}^{\mathrm{div}}(x_1,x_2) = \frac{1}{4}\,\mathrm{curl}\big(\psi_1(2^{j_1}x_1-k_1)\psi_1(2^{j_2}x_2-k_2)\big) = \left| \begin{array}{l} 2^{j_2}\psi_1(2^{j_1}x_1-k_1)\psi_0(2^{j_2}x_2-k_2) \\ -2^{j_1}\psi_0(2^{j_1}x_1-k_1)\psi_1(2^{j_2}x_2-k_2) \end{array} \right. .$$

Here $\mathbf{j}=(j_1,j_2)\in\mathbb{Z}^2$ is the scale parameter, and $\mathbf{k}=(k_1,k_2)\in\mathbb{Z}^2$ the position parameter. For $\mathbf{j},\mathbf{k}\in\mathbb{Z}^2$, the set $\{\Psi_{\mathbf{j},\mathbf{k}}^{\mathrm{div}}\}$ forms a Riesz basis of $\mathbf{H}_{\mathrm{div}\,0}(\mathbb{R}^2)$.

In [8], in contrast to the strategies adopted in previous works, the decomposition algorithm in this divergence-free basis relies on the definition of complementary wavelets. These complementary wavelets supplement the divergence-free wavelets to form a basis of $(L^2(\mathbb{R}^2))^2$:

$$\Psi_{\mathbf{j},\mathbf{k}}^{\mathfrak{N}}(x_1,x_2) = \left| \begin{array}{l} 2^{j_1}\psi_1(2^{j_1}x_1-k_1)\psi_0(2^{j_2}x_2-k_2) \\ 2^{j_2}\psi_0(2^{j_1}x_1-k_1)\psi_1(2^{j_2}x_2-k_2) \end{array} \right. .$$

This choice ensures that, for fixed $\mathbf{j}$ and $\mathbf{k}$, the complementary function $\Psi_{\mathbf{j},\mathbf{k}}^{\mathfrak{N}}$ is orthogonal to the divergence-free wavelet $\Psi_{\mathbf{j},\mathbf{k}}^{\mathrm{div}}$. The exponent $\mathfrak{N}$ (and further $\mathcal{N}$) stands for "normal". Note that imposing this constraint of orthogonality yields a unique solution for the complementary function, contrarily to the several possible choices for the natural supplementary spaces introduced by Urban in [27].

To compute the expansion of any vector field $\mathbf{u}$ into this new basis, we begin with the standard tensor-product wavelet decomposition of $\mathbf{u}$ in the MRA $(V_{j_1}^1 \otimes V_{j_2}^0) \times (V_{j_1}^0 \otimes V_{j_2}^1)$:

$$\mathbf{u} = \sum_{\mathbf{j}\in\mathbb{Z}^2}\sum_{\mathbf{k}\in\mathbb{Z}^2}\big(d_{1,\mathbf{j},\mathbf{k}}\Psi_{\mathbf{j},\mathbf{k}}^1 + d_{2,\mathbf{j},\mathbf{k}}\Psi_{\mathbf{j},\mathbf{k}}^2\big),$$

where for $\mathbf{j},\mathbf{k}\in\mathbb{Z}^2$:

$$\Psi_{\mathbf{j},\mathbf{k}}^1(x_1,x_2) = \left| \begin{array}{l} \psi_1(2^{j_1}x_1-k_1)\psi_0(2^{j_2}x_2-k_2) \\ 0 \end{array} \right. ,$$

$$\Psi_{\mathbf{j},\mathbf{k}}^2(x_1,x_2) = \left| \begin{array}{l} 0 \\ \psi_0(2^{j_1}x_1-k_1)\psi_1(2^{j_2}x_2-k_2) \end{array} \right.$$

are the tensor-product wavelets for each component (in L^∞ normalization).

We can now express $\mathbf{u}$ in terms of the divergence-free wavelet basis and its complementary wavelet basis:

$$\mathbf{u} = \sum_{\mathbf{j}\in\mathbb{Z}^2}\sum_{\mathbf{k}\in\mathbb{Z}^2}\big(d_{\mathrm{div}\,\mathbf{j},\mathbf{k}}\Psi_{\mathbf{j},\mathbf{k}}^{\mathrm{div}} + d_{\mathfrak{N}\,\mathbf{j},\mathbf{k}}\Psi_{\mathbf{j},\mathbf{k}}^{\mathfrak{N}}\big) \tag{1.2}$$

which provides directly the coefficients $d_{\mathrm{div}\,\mathbf{j},\mathbf{k}}$ and $d_{\mathfrak{N}\,\mathbf{j},\mathbf{k}}$:

$$\begin{bmatrix} d_{\mathrm{div}\,\mathbf{j},\mathbf{k}} \\ d_{\mathfrak{N}\,\mathbf{j},\mathbf{k}} \end{bmatrix} = \begin{bmatrix} \frac{2^{j_2}}{2^{2j_1}+2^{2j_2}} & -\frac{2^{j_1}}{2^{2j_1}+2^{2j_2}} \\ \frac{2^{j_1}}{2^{2j_1}+2^{2j_2}} & \frac{2^{j_2}}{2^{2j_1}+2^{2j_2}} \end{bmatrix} \begin{bmatrix} d_{1,\mathbf{j},\mathbf{k}} \\ d_{2,\mathbf{j},\mathbf{k}} \end{bmatrix}. \tag{1.3}$$

Remark 1.1. Since the choice of the complementary wavelets $\Psi_{\mathbf{j},\mathbf{k}}^{\mathfrak{N}}$ is not unique, it influences the values of the coefficients $d_{\mathrm{div}\,\mathbf{j},\mathbf{k}}$ and $d_{\mathfrak{N}\,\mathbf{j},\mathbf{k}}$. We will see in Section 2.3 that this choice also influences the convergence of the wavelet Helmholtz decomposition. Of course, if $\mathbf{u}$ is divergence-free we find $d_{\mathfrak{N}\,\mathbf{j},\mathbf{k}}=0$.

1.2.2. Bivariate curl-free wavelets

The construction of curl-free wavelets in two dimensions is given by considering the gradient of the tensor-product wavelets of the MRA $(V^1_{j_1} \otimes V^1_{j_2})$:

$$\Psi^{\text{curl}}_{\mathbf{j},\mathbf{k}}(x_1,x_2) = \frac{1}{4}\nabla\big(\psi_1(2^{j_1}x_1-k_1)\psi_1(2^{j_2}x_2-k_2)\big) = \left| \begin{array}{l} 2^{j_1}\psi_0(2^{j_1}x_1-k_1)\psi_1(2^{j_2}x_2-k_2) \\ 2^{j_2}\psi_1(2^{j_1}x_1-k_1)\psi_0(2^{j_2}x_2-k_2) \end{array}\right. .$$

These vector wavelets form a basis of the space $\mathbf{H}_{\text{curl}\,0}(\mathbb{R}^2)$. These curl-free wavelets are supplement by the following complementary functions to form a basis for $(L^2(\mathbb{R}^2))^2$:

$$\Psi^{\mathcal{N}}_{\mathbf{j},\mathbf{k}}(x_1,x_2) = \left| \begin{array}{l} 2^{j_2}\psi_0(2^{j_1}x_1-k_1)\psi_1(2^{j_2}x_2-k_2) \\ -2^{j_1}\psi_1(2^{j_1}x_1-k_1)\psi_0(2^{j_2}x_2-k_2) \end{array}\right. .$$

The expansion of any vector field into this wavelet basis can be obtained from the standard decomposition into the canonical wavelets:

$$\mathbf{u} = \sum_{\mathbf{j}\in\mathbb{Z}^2}\sum_{\mathbf{k}\in\mathbb{Z}^2}\big(d_{1,\mathbf{j},\mathbf{k}}\Psi^{\#}_{1,\mathbf{j},\mathbf{k}} + d_{2,\mathbf{j},\mathbf{k}}\Psi^{\#}_{2,\mathbf{j},\mathbf{k}}\big)$$

with

$$\Psi^{\#}_{1,\mathbf{j},\mathbf{k}}(x_1,x_2) = \left| \begin{array}{l} \psi_0(2^{j_1}x_1-k_1)\psi_1(2^{j_2}x_2-k_2) \\ 0 \end{array}\right. , \qquad \Psi^{\#}_{2,\mathbf{j},\mathbf{k}}(x_1,x_2) = \left| \begin{array}{l} 0 \\ \psi_1(2^{j_1}x_1-k_1)\psi_0(2^{j_2}x_2-k_2) \end{array}\right. .$$

The new decomposition:

$$\mathbf{u} = \sum_{\mathbf{j}\in\mathbb{Z}^2}\sum_{\mathbf{k}\in\mathbb{Z}^2}\big(d_{\text{curl}\,\mathbf{j},\mathbf{k}}\Psi^{\text{curl}}_{\mathbf{j},\mathbf{k}} + d_{\mathcal{N}\,\mathbf{j},\mathbf{k}}\Psi^{\mathcal{N}}_{\mathbf{j},\mathbf{k}}\big) \tag{1.4}$$

is thus given by:

$$\begin{bmatrix} d_{\mathcal{N}\,\mathbf{j},\mathbf{k}} \\ d_{\text{curl}\,\mathbf{j},\mathbf{k}} \end{bmatrix} = \begin{bmatrix} \frac{2^{j_2}}{2^{2j_1}+2^{2j_2}} & -\frac{2^{j_1}}{2^{2j_1}+2^{2j_2}} \\ \frac{2^{j_1}}{2^{2j_1}+2^{2j_2}} & \frac{2^{j_2}}{2^{2j_1}+2^{2j_2}} \end{bmatrix} \begin{bmatrix} d_{1,\mathbf{j},\mathbf{k}} \\ d_{2,\mathbf{j},\mathbf{k}} \end{bmatrix}. \tag{1.5}$$

Remark 1.2. One can notice the similarity between the divergence-free and curl-free transforms, emphasized by the equality of matrices in (1.3) and (1.5).

These constructions will be generalized to arbitrary dimension n in the next section.

1.3. Anisotropic divergence-free wavelets adapted to the Leray projector, and associated curl-free and complementary wavelets

1.3.1. Divergence-free wavelets in dimension n

The first and natural idea (also proposed in [16]) for the general form of divergence-free wavelets in dimension n is to introduce:

$$\Psi^{\text{div}\,i}_{\mathbf{j},\mathbf{k}}(x_1,x_2,\dots,x_n) = \begin{array}{r} \\ \\ \\ \text{line } i\rightarrow \\ \\ \\ \text{line } i+1\rightarrow \\ \\ \\ \\ \\ \end{array} \left| \begin{array}{l} 0 \\ \vdots \\ 0 \\ 2^{j_{i+1}}\psi_0(2^{j_1}x_1-k_1)\dots\psi_0(2^{j_{i-1}}x_{i-1}-k_{i-1})\psi_1(2^{j_i}x_i-k_i) \\ \quad\times\psi_0(2^{j_{i+1}}x_{i+1}-k_{i+1})\dots\psi_0(2^{j_n}x_n-k_n) \\ \\ -2^{j_i}\psi_0(2^{j_1}x_1-k_1)\dots\psi_0(2^{j_i}x_i-k_i)\psi_1(2^{j_{i+1}}x_{i+1}-k_{i+1}) \\ \quad\times\psi_0(2^{j_{i+2}}x_{i+2}-k_{i+2})\dots\psi_0(2^{j_n}x_n-k_n) \\ 0 \\ \vdots \\ 0 \end{array}\right. \tag{1.6}$$

for $1 \leqslant i \leqslant n$ (for $i=n$, the line $n+1$ is shifted to the first line and the index j_{n+1} is replaced by j_1). Choosing $n-1$ vector wavelets among these n wavelets allows to form a basis of $\mathbf{H}_{\text{div}\,0}(\mathbb{R}^n)$. In 3D, these wavelets can also be seen as the curl of a function. But for $n \geqslant 4$, these wavelets are no longer derived from the curl operator since the curl operator takes a complicated form.

The complementary functions are chosen to satisfy an orthogonality condition with the divergence-free wavelets of same index $(\mathbf{j},\mathbf{k})$:

$$\Psi^{\mathfrak{N}}_{\mathbf{j},\mathbf{k}}(x_1,x_2,\dots,x_n)=\left|\begin{array}{l}2^{j_1}\psi_1(2^{j_1}x_1-k_1)\psi_0(2^{j_2}x_2-k_2)\dots\psi_0(2^{j_n}x_n-k_n)\\ \vdots\\ 2^{j_i}\psi_0(2^{j_1}x_1-k_1)\dots\psi_1(2^{j_i}x_i-k_i)\dots\psi_0(2^{j_n}x_n-k_n)\\ \vdots\\ 2^{j_n}\psi_0(2^{j_1}x_1-k_1)\psi_0(2^{j_2}x_2-k_2)\dots\psi_1(2^{j_n}x_n-k_n)\end{array}\right. . \tag{1.7}$$

Like in dimension two, the anisotropic divergence-free wavelet transform will be related to the standard anisotropic wavelet transform. Each component u_i of a vector field $\mathbf{u}$ is expanded into the tensor-product wavelet basis of the MRA $(V^0_{j_1}\otimes\dots\otimes V^1_{j_i}\otimes\dots\otimes V^0_{j_n})$:

$$u_i(x_1,\dots,x_n)=\sum_{\mathbf{j},\mathbf{k}\in\mathbb{Z}^n}d_{i\,\mathbf{j},\mathbf{k}}\psi_0\big(2^{j_1}x_1-k_1\big)\dots\psi_1\big(2^{j_i}x_i-k_i\big)\dots\psi_0\big(2^{j_n}x_n-k_n\big).$$

The divergence-free and complementary coefficients of $\mathbf{u}$ are given by:

$$\mathbf{u}=\sum_{i=1}^{n}\sum_{\mathbf{j}\in\mathbb{Z}^n}\sum_{\mathbf{k}\in\mathbb{Z}^n}d_{\mathrm{div}\,i,\mathbf{j},\mathbf{k}}\Psi^{\mathrm{div}\,i}_{\mathbf{j},\mathbf{k}}+\sum_{\mathbf{j}\in\mathbb{Z}^n}\sum_{\mathbf{k}\in\mathbb{Z}^n}d_{\mathfrak{N}\,\mathbf{j},\mathbf{k}}\Psi^{\mathfrak{N}}_{\mathbf{j},\mathbf{k}} \tag{1.8}$$

to which we add the following relationship between divergence-free coefficients:

$$\sum_{i=1}^{n}2^{-j_i-j_{i+1}}d_{\mathrm{div}\,i,\mathbf{j},\mathbf{k}}=0$$

(with the convention $j_{n+1}=j_1$) chosen such that the last row of the matrix in the system below is orthogonal to the others:

$$\begin{bmatrix}2^{j_2}&0&0&\dots&\dots&0&-2^{j_n}&2^{j_1}\\-2^{j_1}&2^{j_3}&0&\ddots&\ddots&\vdots&0&2^{j_2}\\0&-2^{j_2}&2^{j_4}&\ddots&\ddots&\ddots&\vdots&2^{j_3}\\\vdots&\ddots&-2^{j_3}&2^{j_5}&\ddots&\ddots&\vdots&\vdots\\\vdots&\ddots&\ddots&\ddots&\ddots&\ddots&\vdots&\vdots\\0&\dots&\dots&0&-2^{j_{n-2}}&2^{j_n}&0&2^{j_{n-1}}\\0&0&\dots&\dots&0&-2^{j_{n-1}}&2^{j_1}&2^{j_n}\\2^{-j_1-j_2}&2^{-j_2-j_3}&2^{-j_3-j_4}&\dots&2^{-j_{n-2}-j_{n-1}}&2^{-j_{n-1}-j_n}&2^{-j_n-j_1}&0\end{bmatrix}\begin{bmatrix}d^{\mathrm{div}}_{1\mathbf{j},\mathbf{k}}\\d^{\mathrm{div}}_{2\mathbf{j},\mathbf{k}}\\\vdots\\\vdots\\\vdots\\d^{\mathrm{div}}_{n-1\,\mathbf{j},\mathbf{k}}\\d^{\mathrm{div}}_{n\mathbf{j},\mathbf{k}}\\d^{\mathfrak{N}}_{\mathbf{j},\mathbf{k}}\end{bmatrix}=\begin{bmatrix}d_{1\,\mathbf{j},\mathbf{k}}\\d_{2\,\mathbf{j},\mathbf{k}}\\\vdots\\\vdots\\\vdots\\d_{n-1\,\mathbf{j},\mathbf{k}}\\d_{n\,\mathbf{j},\mathbf{k}}\\0\end{bmatrix}. \tag{1.9}$$

Unfortunately, this matrix cannot be made orthogonal for $n\geqslant 4$ even with the choice of the last line orthogonal to the others. However for $n=3$, the matrix of coordinate change is still orthogonal:

$$M=\begin{bmatrix}2^{j_2}&0&-2^{j_3}&2^{j_1}\\-2^{j_1}&2^{j_3}&0&2^{j_2}\\0&-2^{j_2}&2^{j_1}&2^{j_3}\\2^{j_3}&2^{j_1}&2^{j_2}&0\end{bmatrix},\quad\text{with } M^{-1}=\frac{1}{2^{2j_1}+2^{2j_2}+2^{2j_3}}\begin{bmatrix}2^{j_2}&-2^{j_1}&0&2^{j_3}\\0&2^{j_3}&-2^{j_2}&2^{j_1}\\-2^{j_3}&0&2^{j_1}&2^{j_2}\\2^{j_1}&2^{j_2}&2^{j_3}&0\end{bmatrix}. \tag{1.10}$$

This lack of orthogonality for $n\geqslant 4$ makes the inversion of the matrix more difficult. This is the reason why we will construct another divergence-free wavelet basis in which this matrix will be orthogonal. Moreover we will see in Section 3.1 that this new construction will be fruitful for a generalization of the method to isotropic and quasi-isotropic wavelets.

The new method that we propose now is inspired by the expression of the Leray projector in Fourier domain. We recall that the n-dimensional Leray projector $\mathbb{P}$ in Fourier space takes the form:

$$\widehat{\mathbb{P}(\mathbf{u})} = \begin{bmatrix} \widehat{u_{\mathrm{div}\,1}} \\ \widehat{u_{\mathrm{div}\,2}} \\ \vdots \\ \vdots \\ \widehat{u_{\mathrm{div}\,n-1}} \\ \widehat{u_{\mathrm{div}\,n}} \end{bmatrix} = \begin{bmatrix} 1-\frac{\xi_1^2}{|\xi|^2} & -\frac{\xi_2\xi_1}{|\xi|^2} & \cdots & \cdots & -\frac{\xi_n\xi_1}{|\xi|^2} \\ -\frac{\xi_1\xi_2}{|\xi|^2} & 1-\frac{\xi_2^2}{|\xi|^2} & \ddots & \ddots & -\frac{\xi_n\xi_2}{|\xi|^2} \\ \vdots & \ddots & \ddots & \ddots & \vdots \\ \vdots & \ddots & \ddots & \ddots & \vdots \\ -\frac{\xi_1\xi_n}{|\xi|^2} & -\frac{\xi_2\xi_n}{|\xi|^2} & \cdots & -\frac{\xi_{n-1}\xi_n}{|\xi|^2} & 1-\frac{\xi_n^2}{|\xi|^2} \end{bmatrix} \begin{bmatrix} \widehat{u_1} \\ \widehat{u_2} \\ \vdots \\ \vdots \\ \widehat{u_{n-1}} \\ \widehat{u_n} \end{bmatrix} \tag{1.11}$$

where $\widehat{u_k}$ denotes the Fourier transform[1] of the kth component u_k of $\mathbf{u}$, on $\mathbb{R}^n$.

By analogy with this expression of the Leray projector, we construct the following divergence-free wavelets (with the same notation as before).

Definition 1.1 *(n-Dimensional divergence-free wavelets).* For $1 \leqslant i \leqslant n$, we define the vector wavelets

$$\Psi_{\mathbf{j},\mathbf{k}}^{\mathrm{div}\,i}(x_1,\ldots,x_n) = \frac{1}{|\omega|^2} \left| \begin{array}{l} -\omega_i\omega_1\psi_1(\omega_1x_1-k_1)\psi_0(\omega_2x_2-k_2)\ldots\psi_0(\omega_nx_n-k_n) \\ \vdots \\ -\omega_i\omega_{i-1}\psi_0(\omega_1x_1-k_1)\ldots\psi_0(\omega_{i-2}x_{i-2}-k_{i-2})\psi_1(\omega_{i-1}x_{i-1}-k_{i-1}) \\ \quad\times\psi_0(\omega_ix_i-k_i)\ldots\psi_0(\omega_nx_n-k_n) \\ (\sum_{\ell\neq i}\omega_\ell^2)\psi_0(\omega_1x_1-k_1)\ldots\psi_0(\omega_{i-1}x_{i-1}-k_{i-1})\psi_1(\omega_ix_i-k_i) \\ \quad\times\psi_0(\omega_{i+1}x_{i+1}-k_{i+1})\ldots\psi_0(\omega_nx_n-k_n) \\ -\omega_i\omega_{i+1}\psi_0(\omega_1x_1-k_1)\ldots\psi_0(\omega_ix_i-k_i)\psi_1(\omega_{i+1}x_{i+1}-k_{i+1}) \\ \quad\times\psi_0(\omega_{i+2}x_{i+2}-k_{i+2})\ldots\psi_0(\omega_nx_n-k_n) \\ \vdots \\ -\omega_i\omega_n\psi_0(\omega_1x_1-k_1)\ldots\psi_0(\omega_{n-1}x_{n-1}-k_{n-1})\psi_1(\omega_nx_n-k_n) \end{array} \right. \tag{1.12}$$

for $\omega_i = 2^{j_i}$ and $|\omega|^2 = \sum_{i=1}^n 2^{2j_i}$, which give a frame for the space $\mathbf{H}_{\mathrm{div}\,0}(\mathbb{R}^n)$.

The complementary vector wavelets are chosen as before (1.7) with the renormalization:

$$\Psi_{\mathbf{j},\mathbf{k}}^{\mathfrak{N}} \mapsto \frac{1}{|\omega|}\Psi_{\mathbf{j},\mathbf{k}}^{\mathfrak{N}}.$$

For this choice of functions, the basis change matrix which allows to compute the standard coefficients $d_{i,\mathbf{j},\mathbf{k}}$ from the divergence-free coefficients $d_{\mathrm{div}\,i,\mathbf{j},\mathbf{k}}$ (like in system (1.9)), rewrites:

$$M = \begin{bmatrix} 1-\frac{\omega_1^2}{|\omega|^2} & -\frac{\omega_2\omega_1}{|\omega|^2} & \cdots & \cdots & -\frac{\omega_n\omega_1}{|\omega|^2} & \frac{\omega_1}{|\omega|} \\ -\frac{\omega_1\omega_2}{|\omega|^2} & 1-\frac{\omega_2^2}{|\omega|^2} & \ddots & \ddots & -\frac{\omega_n\omega_2}{|\omega|^2} & \frac{\omega_2}{|\omega|} \\ \vdots & \ddots & \ddots & \ddots & \vdots & \vdots \\ \vdots & \ddots & \ddots & \ddots & \vdots & \vdots \\ -\frac{\omega_1\omega_n}{|\omega|^2} & -\frac{\omega_2\omega_n}{|\omega|^2} & \cdots & -\frac{\omega_{n-1}\omega_n}{|\omega|^2} & 1-\frac{\omega_n^2}{|\omega|^2} & \frac{\omega_n}{|\omega|} \\ \frac{\omega_1}{|\omega|} & \frac{\omega_2}{|\omega|} & \cdots & \frac{\omega_{n-1}}{|\omega|} & \frac{\omega_n}{|\omega|} & 0 \end{bmatrix} \tag{1.13}$$

and it is now a symmetric orthogonal matrix ($M^{-1} = M^T = M$).

Remark the analogy between matrices (1.13) and (1.11). Remark also that these new divergence-free wavelets are linear combinations of the previous ones (1.6). Then, the projection onto the divergence-free space generated by divergence-free wavelets of same index $(\mathbf{j},\mathbf{k})$ is the same in both cases. The interest of this new formulation for the basis functions lies in the easy inversion of the matrix M (1.13). It allows to deduce the divergence-free and complementary wavelet coefficients from the standard ones without solving a linear system.

1.3.2. Curl-free wavelets in dimension n

The n-dimensional curl-free vector wavelets are constructed by taking the gradient of the tensor-product wavelets of the MRA $(V_{j_1}^1 \otimes \cdots \otimes V_{j_n}^1)$:

[1] The Fourier transform of a function $f \in L^1(\mathbb{R})$ is noted $\hat{f}(\xi) = \int_{-\infty}^{+\infty} f(x)e^{-ix\xi}\,dx$, we recall that $f \mapsto \frac{1}{\sqrt{2\pi}}\hat{f}$ defines an isometry on $L^2(\mathbb{R})$.

$$\Psi^{\mathrm{curl}}_{\mathbf{j},\mathbf{k}}(x_1,\ldots,x_n)=\frac{1}{4}\nabla\big(\psi_1\big(2^{j_1}x_1-k_1\big)\ldots\psi_1\big(2^{j_n}x_n-k_n\big)\big)$$
$$=\left|\begin{array}{l}2^{j_1}\psi_0(2^{j_1}x_1-k_1)\psi_1(2^{j_2}x_2-k_2)\ldots\psi_1(2^{j_n}x_n-k_n)\\ \vdots\\ 2^{j_i}\psi_1(2^{j_1}x_1-k_1)\ldots\psi_0(2^{j_i}x_i-k_i)\ldots\psi_1(2^{j_n}x_n-k_n)\\ \vdots\\ 2^{j_n}\psi_1(2^{j_1}x_1-k_1)\psi_1(2^{j_2}x_2-k_2)\ldots\psi_0(2^{j_n}x_n-k_n)\end{array}\right. . \tag{1.14}$$

In this case, the complementary wavelets (which will correspond to imperfect divergence-free wavelets) are defined like the anisotropic divergence-free wavelets (1.12), simply by exchanging the 0's and the 1's in the wavelet indices.

2. Orthogonal wavelet Helmholtz decomposition: convergence of an iterative algorithm

The objective now is to compute the Helmholtz decomposition of any vector field $\mathbf{u}$, using divergence-free and curl-free wavelets. More precisely: let $\mathbb{P}$ be the Leray projector and $\mathbb{Q}$ be the orthogonal projector onto the curl-free vector functions, we want to rewrite Eq. (0.1):

$$\mathbf{u}=\mathbb{P}\mathbf{u}+\mathbb{Q}\mathbf{u},\quad \mathbb{P}\mathbf{u}=\mathbf{u}_{\mathrm{div}},\ \ \mathbb{Q}\mathbf{u}=\mathbf{u}_{\mathrm{curl}} \tag{2.1}$$

such that $\mathbf{u}_{\mathrm{div}}$ and $\mathbf{u}_{\mathrm{curl}}$ should be expanded into the divergence-free and curl-free wavelet bases:

$$\mathbf{u}_{\mathrm{div}}=\mathbb{P}\mathbf{u}=\sum_{i,\mathbf{j},\mathbf{k}}d_{\mathrm{div}\,i,\mathbf{j},\mathbf{k}}\Psi^{\mathrm{div}\,i}_{\mathbf{j},\mathbf{k}}\quad\text{and}\quad \mathbf{u}_{\mathrm{curl}}=\mathbb{Q}\mathbf{u}=\sum_{\mathbf{j},\mathbf{k}}d_{\mathrm{curl}\,\mathbf{j},\mathbf{k}}\Psi^{\mathrm{curl}}_{\mathbf{j},\mathbf{k}}. \tag{2.2}$$

However, the divergence-free wavelet basis as well as the curl-free wavelet basis are not orthogonal bases. Then their associated projectors are oblique and depend on the choice of the complement spaces $\mathrm{H}_{\mathfrak{N}}=Span\{\Psi_{\mathfrak{N}}\}$ and $\mathrm{H}_{\mathcal{N}}=Span\{\Psi_{\mathcal{N}}\}$ introduced in Section 1. Therefore we will introduce below an iterative algorithm to provide in practice such a decomposition.

2.1. Iterative computation of divergence-free and curl-free components of any vector field

Our iterative algorithm is based on the following two non-orthogonal decompositions:

$$\big(L^2\big(\mathbb{R}^n\big)\big)^n=\mathbf{H}_{\mathrm{div}\,0}\oplus\mathrm{H}_{\mathfrak{N}}\quad\text{and}\quad\big(L^2\big(\mathbb{R}^n\big)\big)^n=\mathrm{H}_{\mathcal{N}}\oplus\mathbf{H}_{\mathrm{curl}\,0}. \tag{2.3}$$

For a vector field $\mathbf{u}\in(L^2(\mathbb{R}^n))^n$, we introduce the splitting of $\mathbf{u}$:

$$\mathbf{u}=\mathrm{P}_{\mathrm{div}}\mathbf{u}+\mathrm{Q}_{\mathfrak{N}}\mathbf{u} \tag{2.4}$$

into the divergence-free wavelet space and its complement $\mathrm{H}_{\mathfrak{N}}$, and

$$\mathbf{u}=\mathrm{P}_{\mathcal{N}}\mathbf{u}+\mathrm{Q}_{\mathrm{curl}}\mathbf{u} \tag{2.5}$$

the splitting of $\mathbf{u}$ into the curl-free wavelet space and its complement $\mathrm{H}_{\mathcal{N}}$.

Iterative algorithm. The decomposition (2.4) allows to extract the divergence-free part of the field $\mathbf{u}$, whereas the decomposition (2.5) allows to extract its curl-free part, both in an approximate way. We propose to apply them successively until the remainder becomes sufficiently close to 0.

Using the same notations as above, and starting from $\mathbf{u}^0=\mathbf{u}$, the first step of our algorithm is:

$$\text{(step 0)}\quad\begin{cases}\mathbf{u}^{1/2}=\mathbf{u}^0-\mathrm{P}_{\mathrm{div}}\mathbf{u}^0=\mathrm{Q}_{\mathfrak{N}}\mathbf{u}^0,\\ \mathbf{u}^1=\mathbf{u}^{1/2}-\mathrm{Q}_{\mathrm{curl}}\mathbf{u}^{1/2}=\mathrm{P}_{\mathcal{N}}\mathbf{u}^{1/2}.\end{cases}$$

The next steps are defined similarly by:

$$\text{(step } p)\quad \mathbf{u}^{p+1}=\mathrm{P}_{\mathcal{N}}\mathrm{Q}_{\mathfrak{N}}\mathbf{u}^p,\quad\forall p\geqslant 1. \tag{2.6}$$

The sequence $\mathbf{u}^p$ defined like this satisfies:

$$\mathbf{u}^p=\underbrace{\mathrm{P}_{\mathrm{div}}\mathbf{u}^p}_{\mathbf{u}^p_{\mathrm{div}}}+\underbrace{\mathrm{Q}_{\mathrm{curl}}\mathrm{Q}_{\mathfrak{N}}\mathbf{u}^p}_{\mathbf{u}^p_{\mathrm{curl}}}+\underbrace{\mathrm{P}_{\mathcal{N}}\mathrm{Q}_{\mathfrak{N}}\mathbf{u}^p}_{\mathbf{u}^{p+1}}. \tag{2.7}$$

Asymptotically, if the sequence $(\mathbf{u}^p)_{p\in\mathbb{N}}$ converges to 0, then the decomposition (2.1) holds with:

$$\mathbf{u}_{\mathrm{div}}=\sum_{p=0}^{+\infty}\mathbf{u}^p_{\mathrm{div}}\quad\text{and}\quad\mathbf{u}_{\mathrm{curl}}=\sum_{p=0}^{+\infty}\mathbf{u}^p_{\mathrm{curl}}.$$

This algorithm was originally designed in dimension two and three in [8], where we proved its convergence for Shannon wavelets. To speed up the convergence, we propose the following improvement.

Convergence acceleration of the method. In order to speed up the convergence of the algorithm, we will propose a Richardson-like acceleration, using a damping factor for the step (2.6). For some well chosen $b>0$, we replace Eq. (2.7): $\mathbf{u}^{p+1}=\mathbf{u}^p-\mathbf{u}^p_{\text{div}}-\mathbf{u}^p_{\text{curl}}$, by:

$$\mathbf{u}^{p+1}=\mathbf{u}^p-\mathbf{u}^p_{\text{div}}-b\mathbf{u}^p_{\text{curl}}.$$

Then, instead of the projector $\mathrm{P}_{\mathcal{N}}$, we will use the operator:

$$\mathrm{P}_{\mathcal{N}b}\mathbf{u}=\mathbf{u}-b\mathrm{Q}_{\text{curl}}\mathbf{u} \tag{2.8}$$

and the step p (2.6) of the algorithm is then replaced by:

$$(\text{step } p')\quad \mathbf{u}^{p+1}=\mathrm{P}_{\mathcal{N}b}\mathrm{Q}_{\mathfrak{N}}\mathbf{u}^p,\quad \forall p\geqslant 0. \tag{2.9}$$

In the next sections, the convergence of the sequence $\mathbf{u}^p$ will be studied: first a convergence result of algorithm (2.6) will be stated in the bivariate case, for all kinds of wavelets. Then in arbitrary dimension, an optimal convergence rate for algorithm (2.9) will be established, in the particular case of Shannon wavelets which have infinite support but whose Fourier transforms are optimally localized.

2.2. Convergence of the algorithm in 2D

In dimension two we will derive below a criterion which, applied to the wavelet ψ_1 and its dual ψ_1^*, will ensure the convergence of the algorithm (2.9).

First, in order to work with general wavelets, we will express the wavelet projectors in terms of Fourier transform. Let Q_j be the biorthogonal projector onto a 1D wavelet space W_j. Then, as indicated in [15], the wavelet level j of a function u:

$$Q_ju(x)=\sum_{k\in\mathbb{Z}}2^j<u\big|\psi^*\big(2^jx-k\big)>\psi\big(2^jx-k\big) \tag{2.10}$$

writes in Fourier domain:

$$\widehat{Q_ju}(\xi)=\left[\sum_{k\in\mathbb{Z}}\widehat{u}\big(\xi+2k\pi 2^j\big)\overline{\widehat{\psi^*}}\left(\frac{\xi}{2^j}+2k\pi\right)\right]\widehat{\psi}\left(\frac{\xi}{2^j}\right). \tag{2.11}$$

In this last expression, the parameter k does not refer to any space localization. It is a frequency shift. We always have $\overline{\widehat{\psi^*}}(\xi)\widehat{\psi}(\xi)\geqslant 0$, whereas $\overline{\widehat{\psi^*}}(\xi+2k\pi)\widehat{\psi}(\xi)$ goes to 0 when $|k|$ is large or when $\xi+2k\pi$ is close to 0.

Notations. Let $W_{\substack{10\\01}\mathbf{j}}$ be the bivariate vector space generated by the wavelet basis $(\psi_{1\,j_1k_1}(x_1)\psi_{0\,j_2k_2}(x_2))_{\mathbf{k}\in\mathbb{Z}^2}$ for the first component, and by $(\psi_{0\,j_1k_1}(x_1)\psi_{1\,j_2k_2}(x_2))_{\mathbf{k}\in\mathbb{Z}^2}$ for the second component. We define the vector space $W_{\substack{01\\10}\mathbf{j}}$ similarly.

Let $Q_{\substack{10\\01}\mathbf{j}}$ be the wavelet projector onto $W_{\substack{10\\01}\mathbf{j}}$, and $Q_{\substack{01\\10}\mathbf{j}}$ the wavelet projector onto $W_{\substack{01\\10}\mathbf{j}}$:

$$\begin{aligned}Q_{\substack{10\\01}\mathbf{j}}:\big(L^2\big(\mathbb{R}^2\big)\big)^2&\to W_{\substack{10\\01}\mathbf{j}},\\ \mathbf{u}&\mapsto\mathbf{u_j}=Q_{\substack{10\\01}\mathbf{j}}\mathbf{u},\\ Q_{\substack{01\\10}\mathbf{j}}:\big(L^2\big(\mathbb{R}^2\big)\big)^2&\to W_{\substack{01\\10}\mathbf{j}},\\ \mathbf{u}&\mapsto\mathbf{u_j}=Q_{\substack{01\\10}\mathbf{j}}\mathbf{u}.\end{aligned}$$

For these projectors, formula (2.11) becomes:

$$\begin{aligned}\widehat{\mathbf{u}}_{\mathbf{j}}(\xi)=\widehat{Q_{\substack{10\\01}\mathbf{j}}\mathbf{u}}(\xi)&=\left[\sum_{\mathbf{k}\in\mathbb{Z}^2}\widehat{\mathbf{u}}\big(\xi+2\mathbf{k}\pi 2^{\mathbf{j}}\big)\overline{\widehat{\Psi^*}}_{\substack{10\\01}}\left(\frac{\xi}{2^{\mathbf{j}}}+2\mathbf{k}\pi\right)\right]\widehat{\Psi}_{\substack{10\\01}}\left(\frac{\xi}{2^{\mathbf{j}}}\right)\\ &=\begin{bmatrix}\sum_{\mathbf{k}\in\mathbb{Z}^2}[\widehat{u}_{1\mathbf{j}}(\xi+2\mathbf{k}\pi 2^{\mathbf{j}})\overline{\widehat{\psi_1^*}}(\frac{\xi_1}{2^{j_1}}+2k_1\pi)\overline{\widehat{\psi_0^*}}(\frac{\xi_2}{2^{j_2}}+2k_2\pi)]\widehat{\psi_1}(\frac{\xi_1}{2^{j_1}})\widehat{\psi_0}(\frac{\xi_2}{2^{j_2}})\\ \sum_{\mathbf{k}\in\mathbb{Z}^2}[\widehat{u}_{2\mathbf{j}}(\xi+2\mathbf{k}\pi 2^{\mathbf{j}})\overline{\widehat{\psi_0^*}}(\frac{\xi_1}{2^{j_1}}+2k_1\pi)\overline{\widehat{\psi_1^*}}(\frac{\xi_2}{2^{j_2}}+2k_2\pi)]\widehat{\psi_0}(\frac{\xi_1}{2^{j_1}})\widehat{\psi_1}(\frac{\xi_2}{2^{j_2}})\end{bmatrix}\end{aligned}$$

with the notation $\xi+2\mathbf{k}\pi 2^{\mathbf{j}}=(\xi_1+2k_1\pi 2^{j_1},\xi_2+2k_2\pi 2^{j_2})$. A similar expression can be obtained for $Q_{\substack{01\\10}\mathbf{j}}$.

These wavelet projectors $Q_{\substack{10\\01}\mathbf{j}}$ and $Q_{\substack{01\\10}\mathbf{j}}$ are necessary to express respectively the projector $\mathrm{Q}_{\mathfrak{N}\mathbf{j}}$ onto the complement $H_{\mathfrak{N}}$ of the divergence-free wavelet space, for a fixed level $\mathbf{j}$, and the projector $\mathrm{P}_{\mathcal{N}\mathbf{j}}$ onto the complement $H_{\mathcal{N}}$ of the curl-free wavelet space, at level $\mathbf{j}$:

$$\widehat{\mathrm{Q}_{\mathfrak{N}\mathbf{j}} Q_{\substack{10\\01}\mathbf{j}}\mathbf{u}}(\xi) = \frac{1}{|\omega|^2}\begin{bmatrix} \omega_1^2 & \omega_1^2\frac{\xi_2}{\xi_1} \\ \omega_2^2\frac{\xi_1}{\xi_2} & \omega_2^2 \end{bmatrix} \widehat{Q_{\substack{10\\01}\mathbf{j}}\mathbf{u}}(\xi)$$

and

$$\widehat{\mathrm{P}_{\mathcal{N}\mathbf{j}} Q_{\substack{01\\10}\mathbf{j}}\mathbf{u}}(\xi) = \frac{1}{|\omega|^2}\begin{bmatrix} \omega_2^2 & -\omega_2^2\frac{\xi_1}{\xi_2} \\ -\omega_1^2\frac{\xi_2}{\xi_1} & \omega_1^2 \end{bmatrix} \widehat{Q_{\substack{01\\10}\mathbf{j}}\mathbf{u}}(\xi)$$

where we have noted $\omega = (\omega_1, \omega_2) = 2^{\mathbf{j}} = (2^{j_1}, 2^{j_2})$.

We remark that the sequence $(\mathbf{u}^p)_{p\geqslant 0}$ introduced in relation (2.6) can be written in terms of the operators above:

$$\mathbf{u}^{p+1} = \sum_{\mathbf{i}\in\mathbb{Z}^2} \mathrm{P}_{\mathcal{N}\mathbf{i}} Q_{\substack{01\\10}\mathbf{i}} \sum_{\mathbf{j}\in\mathbb{Z}^2} \mathrm{Q}_{\mathfrak{N}\mathbf{j}} Q_{\substack{10\\01}\mathbf{j}} \mathbf{u}^p.$$

Now let us define the sequence $(\mathbf{v}^q)_{q\geqslant 0}$ as follows:

$$\mathbf{v}^0 = \mathbf{u}^0 = \mathbf{u}$$

and for $q \geqslant 0$,

$$\widehat{\mathbf{v}}^{q+1} = \sum_{\mathbf{j}\in\mathbb{Z}^2} \frac{\omega_1\omega_2}{|\omega|^2}\left(\frac{\xi_2\omega_1}{\omega_2\xi_1} - \frac{\xi_1\omega_2}{\omega_1\xi_2}\right)\left[\sum_{\mathbf{k}\in\mathbb{Z}^2} \widehat{\mathbf{v}}^q\left(\xi + 2\mathbf{k}\pi 2^{\mathbf{j}}\right)\overline{\widehat{\Psi^*}}_{\substack{10\\01}}\left(\frac{\xi}{2^{\mathbf{j}}} + 2\mathbf{k}\pi\right)\right]\widehat{\Psi}_{\substack{10\\01}}\left(\frac{\xi}{2^{\mathbf{j}}}\right). \tag{2.12}$$

Lemma 2.1. *Let the sequence $(\mathbf{v}^q)_{q\geqslant 0}$ be defined by $\mathbf{v}^0 = \mathbf{u}$ and (2.12). Then the sequence $\mathbf{u}^p$ defined by $\mathbf{u}^0 = \mathbf{u}$ and $\mathbf{u}^{p+1/2} = \mathrm{Q}_{\mathfrak{N}}\mathbf{u}^p$, $\mathbf{u}^{p+1} = \mathrm{P}_{\mathcal{N}}\mathrm{Q}_{\mathfrak{N}}\mathbf{u}^p$ for $p \geqslant 0$, fulfill the relations*:

$$\widehat{\mathbf{u}}^{p+1/2}(\xi) = -\sum_{\mathbf{j}\in\mathbb{Z}^2} \frac{1}{|\omega|^2}\begin{bmatrix} \frac{\omega_1^2}{\xi_1} \\ \frac{\omega_2^2}{\xi_2} \end{bmatrix}\begin{bmatrix} \xi_1 & \xi_2 \end{bmatrix}\widehat{Q_{\substack{10\\01}\mathbf{j}}\mathbf{v}^{2p}}(\xi) \tag{2.13}$$

and

$$\widehat{\mathbf{u}}^{p+1}(\xi) = \sum_{\mathbf{j}\in\mathbb{Z}^2} \frac{\omega_1\omega_2}{|\omega|^2}\begin{bmatrix} \frac{\xi_1}{\omega_1^2} \\ -\frac{\xi_2}{\omega_2^2} \end{bmatrix}\begin{bmatrix} \frac{\omega_1\omega_2}{\xi_2} & \frac{\omega_1\omega_2}{\xi_1} \end{bmatrix}\widehat{Q_{\substack{10\\01}\mathbf{j}}\mathbf{v}^{2p+1}}(\xi). \tag{2.14}$$

The proof of this lemma is not reported here. It uses the expression of the wavelet operators introduced in this part, together with the relations $i\xi\widehat{\psi_1}(\xi) = 4\widehat{\psi_0}(\xi)$ and $i\xi\widehat{\psi_0^*}(\xi) = -4\widehat{\psi_1^*}(\xi)$.

As the operators (2.13) and (2.14) are continuous, to prove the convergence of the Helmholtz algorithm we just have to prove that the sequence $(\mathbf{v}^q)_{q\geqslant 0}$ defined by (2.12) tends to 0. Therefore we will provide the following criterium of convergence:

Theorem 2.1. *The L^2-convergence of the wavelet Helmholtz algorithm is equivalent to*: *for all $f \in L^2(\mathbb{R}^2)$, the sequence $(f^q)_{q\geqslant 0}$ defined by $f^0 = f$ and*

$$f^{q+1}(\xi) = \sum_{\mathbf{j}\in\mathbb{Z}^2} \frac{\omega_1\omega_2}{|\omega|^2}\left(\frac{\xi_2\omega_1}{\omega_2\xi_1} - \frac{\xi_1\omega_2}{\omega_1\xi_2}\right)\left[\sum_{\mathbf{k}\in\mathbb{Z}^2} f^q\left(\xi + 2\mathbf{k}\pi 2^{\mathbf{j}}\right)\overline{\widehat{\Psi^*}}_{10}\left(\frac{\xi}{2^{\mathbf{j}}} + 2\mathbf{k}\pi\right)\right]\widehat{\Psi}_{10}\left(\frac{\xi}{2^{\mathbf{j}}}\right) \tag{2.15}$$

for $q \geqslant 0$, $\xi \in \mathbb{R}^2$, converge to 0 in L^2-norm.

To prove this theorem, we use the symmetry between the variables ξ_1 and ξ_2 and the fact that the two components of the sequence $(\widehat{\mathbf{v}}^q)$ do not interact.

We denote by $f^{q+1} = Qf^q$ the relation (2.15).

Now, we prove the convergence of the sequence $(f^q)_{q\geqslant 0}$ in L^1-norm under some condition on ψ_1 and ψ_1^*. This convergence will give the convergence of the Helmholtz algorithm in L^∞-norm.

Theorem 2.2. *Let D be a set such that $\bigcup_{m\in\mathbb{Z}} 2^m D = \mathbb{R}^2 \setminus \{(0,0)\}$, for instance $D = [-2\pi, 2\pi]^2 \setminus [-\pi, \pi]^2$, and $\Theta = \{\theta \in \mathbb{Q}^2$ s.t. $\exists m, \ell \in \mathbb{Z}^2,\ \theta = (2^{m_1}\ell_1, 2^{m_2}\ell_2)\}$. Then, if $\exists \rho < 1$ such that $\forall \zeta \in D$, the function $\rho(\zeta)$ defined by:*

$$\rho(\zeta) = \sum_{\theta\in\Theta}\Bigg| \sum_{\mathbf{j},\mathbf{k}\in\mathbb{Z}^2,\, 2^{\mathbf{j}}\mathbf{k}=\theta} \frac{\omega_1\omega_2}{|\omega|^2}\left(\frac{(\zeta_2-2\pi\theta_2)\omega_1}{\omega_2(\zeta_1-2\pi\theta_1)} - \frac{(\zeta_1-2\pi\theta_1)\omega_2}{\omega_1(\zeta_2-2\pi\theta_2)}\right)\frac{\zeta_2-2\pi\theta_2}{\zeta_2} \times \overline{\widehat{\psi_1^*}}\left(\frac{\zeta_1}{2^{j_1}}\right)\overline{\widehat{\psi_1^*}}\left(\frac{\zeta_2}{2^{j_2}}\right)\widehat{\psi_1}\left(\frac{\zeta_1-2\pi\theta_1}{2^{j_1}}\right)\widehat{\psi_1}\left(\frac{\zeta_2-2\pi\theta_2}{2^{j_2}}\right)\Bigg| \tag{2.16}$$

with $\omega = 2^{\mathbf{j}}$, verifies $\rho(\zeta) \leqslant \rho$, then the wavelet Helmholtz decomposition algorithm converges.

Proof. Let $f \in L^1(\mathbb{R}^2)$. Then Eq. (2.15) provides:

$$\|Qf\|_{L^1} = \int_{\xi\in\mathbb{R}^2}\Bigg| \sum_{\mathbf{j}\in\mathbb{Z}^2,\,\omega=2^{\mathbf{j}}} \frac{\omega_1\omega_2}{|\omega|^2}\left(\frac{\xi_2\omega_1}{\omega_2\xi_1} - \frac{\xi_1\omega_2}{\omega_1\xi_2}\right) \times\left[\sum_{\mathbf{k}\in\mathbb{Z}^2} f\big(\xi + 2\mathbf{k}\pi 2^{\mathbf{j}}\big)\overline{\widehat{\psi_1^*}}\left(\frac{\xi_1}{2^{j_1}} + 2k_1\pi\right)\overline{\widehat{\psi_0^*}}\left(\frac{\xi_2}{2^{j_2}} + 2k_2\pi\right)\right]\widehat{\psi_1}\left(\frac{\xi_1}{2^{j_1}}\right)\widehat{\psi_0}\left(\frac{\xi_2}{2^{j_2}}\right)\Bigg|\,d\xi.$$

We invert the sums in order to isolate the function f in the expression:

$$\|Qf\|_{L^1} \leqslant \int_{\xi\in\mathbb{R}^2}\sum_{\theta\in\Theta}\Bigg| \sum_{\mathbf{j},\mathbf{k}\in\mathbb{Z}^2,\,2^{\mathbf{j}}\mathbf{k}=\theta} \frac{\omega_1\omega_2}{|\omega|^2}\left(\frac{\xi_2\omega_1}{\omega_2\xi_1} - \frac{\xi_1\omega_2}{\omega_1\xi_2}\right) \times \overline{\widehat{\psi_1^*}}\left(\frac{\xi_1+2\pi\theta_1}{2^{j_1}}\right)\overline{\widehat{\psi_0^*}}\left(\frac{\xi_2+2\pi\theta_2}{2^{j_2}}\right)\widehat{\psi_1}\left(\frac{\xi_1}{2^{j_1}}\right)\widehat{\psi_0}\left(\frac{\xi_2}{2^{j_2}}\right)\Bigg|\big|f(\xi+2\pi\theta)\big|\,d\xi.$$

Using the monotone convergence theorem and the change of variables $\zeta = \xi + 2\pi\theta$ leads to:

$$\|Qf\|_{L^1} \leqslant \sum_{\theta\in\Theta}\int_{\zeta\in\mathbb{R}^2}\Bigg| \sum_{\mathbf{j},\mathbf{k}\in\mathbb{Z}^2,\,2^{\mathbf{j}}\mathbf{k}=\theta} \frac{\omega_1\omega_2}{|\omega|^2}\left(\frac{(\zeta_2-2\pi\theta_2)\omega_1}{\omega_2(\zeta_1-2\pi\theta_1)} - \frac{(\zeta_1-2\pi\theta_1)\omega_2}{\omega_1(\zeta_2-2\pi\theta_2)}\right) \times \overline{\widehat{\psi_1^*}}\left(\frac{\zeta_1}{2^{j_1}}\right)\overline{\widehat{\psi_0^*}}\left(\frac{\zeta_2}{2^{j_2}}\right)\widehat{\psi_1}\left(\frac{\zeta_1-2\pi\theta_1}{2^{j_1}}\right)\widehat{\psi_0}\left(\frac{\zeta_2-2\pi\theta_2}{2^{j_2}}\right)\Bigg|\big|f(\zeta)\big|\,d\xi.$$

Transforming ψ_0 and ψ_0^* into ψ_1 and ψ_1^* thanks to the relations $i\xi\widehat{\psi_1}(\xi) = 4\widehat{\psi_0}(\xi)$ and $i\xi\widehat{\psi_0^*}(\xi) = -4\widehat{\psi_1^*}(\xi)$ makes apparent the function $\rho(\zeta)$ as it was defined by Eq. (2.16). Then, exchanging the sum and the integral, we obtain:

$$\|Qf\|_{L^1} \leqslant \int_{\zeta\in\mathbb{R}^2}\rho(\zeta)\big|f(\zeta)\big|\,d\xi.$$

Hence, if the condition $\rho(\zeta) \leqslant \rho < 1$ is satisfied, we get $\|Qf\|_{L^1} \leqslant \rho\|f\|_{L^1}$, and the sequence $(f^q)_{q\geqslant 0}$ defined by (2.15) converges to 0 in L^1-norm, which means that its Fourier transform converges to 0 in L^∞-norm.

From Theorem 2.1, we may say that the most important feature is the localization of the Fourier spectra of functions ψ_0, ψ_1, ψ_0^* and ψ_1^*. Numerical experiments [6] corroborate this assertion and show that the convergence rate of the Helmholtz algorithm improves when the order of the wavelet basis increases. We can also notice that the horizontal wavelet conditioning (i.e. the scalar products $\langle\psi_{jk}, \psi_{jk'}\rangle$ for a fixed j) does not play any rôle in the convergence of the algorithm.

The computation of ρ in the case of Shannon wavelets (see their definition in the next section) gives $\rho = 3/4$ which is in agreement with the results of part 2.3 for $b = 1$. It is also possible to compute ρ numerically in the case of Meyer wavelets (see for instance [19]), since if we take $D = [-\frac{4}{3}\pi, \frac{4}{3}\pi]^2 \setminus [-\frac{2}{3}\pi, \frac{2}{3}\pi]^2$, the sum over θ contains four terms, containing itself four terms in the sum over $\mathbf{k}, \mathbf{j}$. More detailed results will be presented in a further work.

The proof of convergence for arbitrary dimension will be done using Shannon wavelets, in Section 2.3. But the localization in Fourier domain of wavelet projectors should allow to generalize the convergence to other wavelets, since expression (2.11) implies:

$$\widehat{Q_j u}(\xi) = w_{u\,j}\left(\frac{\xi}{2^j}\right)\widehat{\psi}\left(\frac{\xi}{2^j}\right) \tag{2.17}$$

with $w_{u\,j}$ a 2π-periodic function. □

2.3. Convergence of the damped wavelet Helmholtz decomposition algorithm using Shannon wavelets

We will study now the convergence rate of the accelerated algorithm (2.9), in arbitrary dimension n, using Shannon wavelets. The Shannon wavelet ψ is compactly supported in Fourier space, and is given by the expression:

$$\widehat{\psi}(\xi) = e^{-i\xi/2}\chi_{[-2\pi,-\pi]\cup[\pi,2\pi]}(\xi), \qquad \psi(x) = \frac{\sin 2\pi(x-1/2)}{\pi(x-1/2)} - \frac{\sin \pi(x-1/2)}{\pi(x-1/2)},$$

where χ stands for the characteristic function, i.e. $\chi_E(x) = 1$ if $x \in E$, $\chi_E(x) = 0$ if $x \notin E$.

The corresponding scaling function is:

$$\hat{\varphi}(\xi) = \chi_{[-\pi,\pi]}(\xi), \qquad \varphi(x) = \frac{\sin \pi x}{\pi x}.$$

Then

$$\forall j,k \in \mathbb{Z}, \quad \mathrm{supp}(\widehat{\psi}_{j,k}) = \left[-2^{j+1}\pi, -2^j\pi\right] \cup \left[2^j\pi, 2^{j+1}\pi\right].$$

This property allows a simplification of the wavelet projection (2.11) which rewrites:

$$\widehat{Q_j u}(\xi) = \widehat{u}(\xi)\chi_{\pm[2^j\pi,2^{j+1}\pi]}(\xi).$$

Theorem 2.3. *Let* $\mathbf{u}$ *in* $(L^2(\mathbb{R}^n))^n$*, and let the sequence* $(\mathbf{u}^p)_{p\geqslant 0}$ *be defined by*:

$$\mathbf{u}^0 = \mathbf{u} \quad \text{and} \quad \mathbf{u}^{p+1} = \mathrm{P}_{\mathcal{N}b}\mathrm{Q}_{\mathfrak{N}}\mathbf{u}^p, \quad p \geqslant 0, \tag{2.18}$$

where $\mathrm{Q}_{\mathfrak{N}}$ *is the complementary projector associated to curl-free wavelets* (2.5)*, and* $\mathrm{P}_{\mathcal{N}b}$ *is the damped complementary projector defined in* (2.8)*, associated to divergence-free wavelets* (2.4)*. We assume that the wavelet* ψ_1 *used for constructing the divergence-free and curl-free wavelets of Section* 1.3 *is the Shannon wavelet.*

Then, for $b = \frac{32}{41}$*, the sequence* $(\mathbf{u}^p)$ *satisfies, in* L^2 *norm*:

$$\left\|\mathbf{u}^p\right\| \leqslant \left(\frac{9}{41}\right)^p \|\mathbf{u}\| \tag{2.19}$$

and converges to zero in L^2.

Moreover, the Helmholtz decomposition (0.1) *of* $\mathbf{u}$ *is given by*:

$$\mathbf{u}_{\mathrm{div}} = \sum_{p\in\mathbb{N}} \mathrm{P}_{\mathrm{div}}\mathbf{u}^p, \qquad \mathbf{u}_{\mathrm{curl}} = \sum_{p\in\mathbb{N}} \mathrm{Q}_{\mathrm{curl}}\mathrm{Q}_{\mathfrak{N}}\mathbf{u}^p.$$

Remark 2.1. This result has to be compared with the convergence rate $(\frac{9}{16})^p$ previously obtained in [9] without any damping factor (proved in the 2D and 3D case, also with Shannon wavelets).

Proof of Theorem 2.3. Let ψ_1 and ψ_0 be two wavelets such that $\psi_1' = 4\psi_0$ as in Proposition 1.1 of Section 1. Then for $j,k \in \mathbb{Z}$:

$$\psi_1\widehat{\left(2^j\cdot -k\right)} = 4\frac{2^j}{i\xi}\psi_0\widehat{\left(2^j\cdot -k\right)}, \quad \text{which gives } \widehat{\psi_{1,j,k}} = \frac{4\omega}{i\xi}\widehat{\psi_{0,j,k}} \quad \text{for } \omega = 2^j.$$

For each $\mathbf{j} \in \mathbb{Z}^n$, we consider the level $\mathbf{j}$ of the wavelet decomposition of a vector field $\mathbf{u}$:

$$\mathbf{u_j} = \left|\begin{array}{l} u_{\mathbf{j}1} = \sum_{\mathbf{k}\in\mathbb{Z}^n} d_{1,\mathbf{j},\mathbf{k}}\psi_{1,j_1,k_1}(x_1)\psi_{0,j_2,k_2}(x_2)\ldots\psi_{0,j_n,k_n}(x_n) \\ \vdots \\ u_{\mathbf{j}i} = \sum_{\mathbf{k}\in\mathbb{Z}^n} d_{i,\mathbf{j},\mathbf{k}}\psi_{0,j_1,k_1}(x_1)\ldots\psi_{1,j_i,k_i}(x_i)\ldots\psi_{0,j_n,k_n}(x_n) \\ \vdots \\ u_{\mathbf{j}n} = \sum_{\mathbf{k}\in\mathbb{Z}^n} d_{1,\mathbf{j},\mathbf{k}}\psi_{0,j_1,k_1}(x_1)\ldots\psi_{0,j_{n-1},k_{n-1}}(x_{n-1})\psi_{1,j_n,k_n}(x_n) \end{array}\right. .$$

Applying the Fourier transform to each component yields for $1 \leqslant i \leqslant n$, with $\omega_i = 2^{j_i}$:

$$\widehat{u_{\mathbf{j}i}} = \sum_{\mathbf{k}\in\mathbb{Z}^n} \frac{4\omega_i}{i\xi_i} d_{i,\mathbf{j},\mathbf{k}}\widehat{\psi_{0,j_1,k_1}}(\xi_1)\ldots\widehat{\psi_{0,j_i,k_i}}(\xi_i)\ldots\widehat{\psi_{0,j_n,k_n}}(\xi_n).$$

Then we obtain the complementary part $\mathrm{Q}_{\mathfrak{N}}\mathbf{u_j}$ of the oblique projection onto the divergence-free wavelet space, by applying the orthogonal matrix (1.13) to the wavelet coefficients, and considering the last component:

$$\widehat{\mathrm{Q}_{\mathfrak{N}}\mathbf{u_j}} = \sum_{\mathbf{k}\in\mathbb{Z}^n}\left(\sum_{i=1}^{n}\frac{\omega_i}{|\omega|}d_{i,\mathbf{j},\mathbf{k}}\right)\frac{1}{|\omega|}\widehat{\Psi^{\mathfrak{N}}_{\mathbf{j},\mathbf{k}}}$$

$$= \sum_{\mathbf{k}\in\mathbb{Z}^n}\left(\sum_{i=1}^{n}\frac{\omega_i}{|\omega|}d_{i,\mathbf{j},\mathbf{k}}\right)\left|\begin{array}{l}\frac{\omega_1}{|\omega|}\widehat{\psi_{1,j_1,k_1}}(\xi_1)\widehat{\psi_{0,j_2,k_2}}(\xi_2)\ldots\widehat{\psi_{0,j_n,k_n}}(\xi_n)\\ \vdots\\ \frac{\omega_\ell}{|\omega|}\widehat{\psi_{0,j_1,k_1}}(\xi_1)\ldots\widehat{\psi_{1,j_\ell,k_\ell}}(\xi_\ell)\ldots\widehat{\psi_{0,j_n,k_n}}(\xi_n)\\ \vdots\\ \frac{\omega_n}{|\omega|}\widehat{\psi_{0,j_1,k_1}}(\xi_1)\ldots\widehat{\psi_{0,j_{n-1},k_{n-1}}}(\xi_{n-1})\widehat{\psi_{1,j_n,k_n}}(\xi_n)\end{array}\right. .$$

$\widehat{\mathrm{Q}_{\mathfrak{N}}\mathbf{u_j}}$ may be expressed in terms of $\widehat{\mathbf{u_j}}$:

$$(\widehat{\mathrm{Q}_{\mathfrak{N}}\mathbf{u_j}})_\ell = \frac{\omega_\ell}{|\omega|^2}\left(\frac{4\omega_\ell}{i\xi_\ell}\right)\sum_{i=1}^{n}\omega_i\sum_{\mathbf{k}\in\mathbb{Z}^n}d_{i,\mathbf{j},\mathbf{k}}\widehat{\psi_{0,j_1,k_1}}(\xi_1)\ldots\widehat{\psi_{0,j_n,k_n}}(\xi_n) = \frac{\omega_\ell^2}{|\omega|^2\xi_\ell}\sum_{i=1}^{n}\xi_i\widehat{u_{\mathbf{j}i}} \tag{2.20}$$

and we can write: $\widehat{\mathrm{Q}_{\mathfrak{N}}\mathbf{u_j}} = A_{\mathfrak{N}}\widehat{\mathbf{u_j}}$, where

$$A_{\mathfrak{N}} = \begin{bmatrix}\frac{\omega_1^2}{|\omega|^2\xi_1}\\ \vdots\\ \frac{\omega_n^2}{|\omega|^2\xi_n}\end{bmatrix}\times[\xi_1\ldots\xi_n].$$

Similarly, we can express the Fourier transform of $\mathrm{P}_{\mathcal{N}b}\mathbf{u_j}$ as $A_{\mathcal{N}b}\widehat{\mathbf{u_j}}$ with:

$$A_{\mathcal{N}b} = Id - b\begin{bmatrix}\xi_1\\ \vdots\\ \xi_n\end{bmatrix}\times\left[\frac{\omega_1^2}{|\omega|^2\xi_1}\ldots\frac{\omega_n^2}{|\omega|^2\xi_n}\right]. \tag{2.21}$$

Since the wavelet basis we use for the application $\mathrm{P}_{\mathcal{N}b}$ differs from the one we use for the projection $\mathrm{Q}_{\mathfrak{N}}$, the level $\mathbf{j}$ of the MRA component $\mathbf{u_j}$ corresponds to two different projections of $\mathbf{u}$ when considering either $\mathrm{P}_{\mathcal{N}b}$, or $\mathrm{Q}_{\mathfrak{N}}$. Accordingly we cannot write in general:

$$\widehat{\mathrm{P}_{\mathcal{N}b}\mathrm{Q}_{\mathfrak{N}}\mathbf{u_j}} = A_{\mathcal{N}b}A_{\mathfrak{N}}\widehat{\mathbf{u_j}} \tag{2.22}$$

since we would have to consider projectors of the type $Q_{\substack{1\ldots0\\ \vdots\ \mathbf{j}\\ 0\ldots1}}$ and $Q_{\substack{0\ldots1\\ \vdots\ \mathbf{i}\\ 1\ldots0}}$ with general wavelets, like in the 2D case discussed in Section 2.2.

For simplicity, we will consider the particular case where the component $\mathbf{u_j}$ is the same for the two decompositions, which means:

$$Q_{\substack{1\ldots0\\ \vdots\ \mathbf{j}\\ 0\ldots1}} = Q_{\substack{0\ldots1\\ \vdots\ \mathbf{j}\\ 1\ldots0}}\quad \forall\mathbf{j}\in\mathbb{Z}^2.$$

This equality is satisfied when using Shannon wavelets. Therefore we will assume now that the function ψ_1 is a Shannon wavelet, and we will establish that (2.22) holds in this context.

When ψ_1 is a Shannon wavelet, the wavelet levels $\widehat{\mathbf{u_j}}$ of the vector function $\mathbf{u}$ have disjoint compact supports. Hence $\mathbf{u}^p_{\mathbf{j}}$, the level $\mathbf{j}$ of the wavelet decomposition of $\mathbf{u}^p$, is stable under the different projections. Eq. (2.22) is valid, also with $\widehat{\mathbf{u}}(\xi)$ instead of $\widehat{\mathbf{u_j}}(\xi)$ under the condition $\xi\in\prod_{i=1}^n\pm(2^{j_i}\pi,2^{j_i+1}\pi)$.

Each iteration $\mathbf{u}^{p+1} = \mathrm{P}_{\mathcal{N}b}\mathrm{Q}_{\mathfrak{N}}\mathbf{u}^p$ of the damped algorithm (2.9) can be written in Fourier:

$$\forall\xi\in\prod_{i=1}^{n}\pm\left(2^{j_i}\pi,2^{j_i+1}\pi\right),\quad \widehat{\mathbf{u}^{p+1}_{\mathbf{j}}}(\xi) = A_{\mathcal{N}b}A_{\mathfrak{N}}\widehat{\mathbf{u}^p_{\mathbf{j}}}(\xi)$$

where the matrix

$$A_{\mathcal{N}b}A_{\mathfrak{N}} = \left(Id - \frac{b}{|\omega|^2}\begin{bmatrix}\xi_1\\ \vdots\\ \xi_n\end{bmatrix}\times\left[\frac{\omega_1^2}{\xi_1}\ldots\frac{\omega_n^2}{\xi_n}\right]\right)\times\frac{1}{|\omega|^2}\begin{bmatrix}\frac{\omega_1^2}{\xi_1}\\ \vdots\\ \frac{\omega_n^2}{\xi_n}\end{bmatrix}\times[\xi_1\ldots\xi_n]$$

is of rank one. Thus it has only one non-zero eigenvalue, noted $\lambda(\xi)$, which can be computed by:

$$\lambda(\xi) = \mathrm{trace}(A_{\mathcal{N}b}A_{\mathfrak{N}}) = 1 - b\left(\sum_{i=1}^{n}\xi_i^2\right)\left(\sum_{i=1}^{n}\frac{\omega_i^4}{|\omega|^4\xi_i^2}\right).$$

Introducing $\zeta_i = \frac{\xi_i}{\omega_i} \in \pm[\pi, 2\pi]$, and $\alpha_i = \frac{\omega_i}{|\omega|}$, we obtain:

$$\lambda(\xi) = 1 - bF(\zeta,\alpha) \quad \text{for } F(\zeta,\alpha) = \left(\sum_{i=1}^{n}\alpha_i^2\zeta_i^2\right)\left(\sum_{i=1}^{n}\alpha_i^2\zeta_i^{-2}\right).$$

Since we are using Shannon wavelets, $|\zeta_i| \in [\pi, 2\pi]$ for $1 \leqslant i \leqslant n$. Under the constraint $\sum_{i=1}^{n}\alpha_i^2 = 1$, the maximization of F is no more than a Kantorovich inequality, which yields for a fixed $\zeta \in \pm[\pi, 2\pi]^n$:

$$\max_{\alpha_i, \sum\alpha_i^2=1} F(\zeta,\alpha) = \frac{1}{4}\left(\frac{\min|\zeta_i|}{\max|\zeta_i|} + \frac{\max|\zeta_i|}{\min|\zeta_i|}\right)^2 = \frac{1}{4}\left(2+\frac{1}{2}\right)^2 = \frac{25}{16}. \tag{2.23}$$

The minimization of F uses the convexity of the function $x \mapsto \frac{1}{x}$ and yields:

$$\min_{\alpha_i, \sum\alpha_i^2=1} F(\zeta,\alpha) = 1.$$

As $1 - b\max F \leqslant \lambda \leqslant 1 - b\min F$, the optimal b is obtained for: $b\max F - 1 = 1 - b\min F$, that means $b = \frac{32}{41}$. For this value of b we obtain:

$$\left|\lambda(\xi)\right| \leqslant \frac{9}{41}.$$

Hence,

$$\forall \xi \in \prod_{i=1}^{n} \pm\left[2^{j_i}\pi, 2^{j_i+1}\pi\right], \quad \left|\widehat{\mathbf{u}_{\mathbf{j}}^{p+1}}(\xi)\right| \leqslant \frac{9}{41}\left|\widehat{\mathbf{u}_{\mathbf{j}}^{p}}(\xi)\right|.$$

As for Shannon wavelets, $\|\mathbf{u}\|_{L^2}^2 = \sum_{\mathbf{j}\in\mathbb{Z}^n}\|\mathbf{u_j}\|_{L^2}^2$, by adding the different levels of the wavelet decomposition, we obtain:

$$\left\|\mathbf{u}^{p+1}\right\|_{L^2} \leqslant \frac{9}{41}\left\|\mathbf{u}^{p}\right\|_{L^2}$$

which leads to the result (2.19) by recursivity.

Finally, we add the divergence-free components and the curl-free components arising from the decomposition (2.7) separately to form the divergence-free part and the curl-free part of $\mathbf{u}$ in the wavelet domain:

$$\mathbf{u}_{\mathrm{div}} = \sum_{p\in\mathbb{N}} \mathrm{P}_{\mathrm{div}}\mathbf{u}^p, \qquad \mathbf{u}_{\mathrm{curl}} = \sum_{p\in\mathbb{N}} \mathrm{Q}_{\mathrm{curl}}\mathrm{Q}_{\mathfrak{N}}\mathbf{u}^p. \qquad \square$$

Remark 2.2. In the numerical experiments of Section 4, we will use a quadratic spline wavelet ψ_1 with one vanishing moment. For this wavelet, the optimal value for b was experimentally founded: $b = 1.24$. For $b = 1.24$, the convergence rate is equal to 0.41 instead of 0.56 for $b = 1$.

3. Generalization of the isotropic divergence-free wavelet construction

Despite the fact that anisotropic wavelets are well suited for image compression, or for the study of anisotropic spaces [13], they are not often used in numerical adaptive schemes. Indeed, isotropic wavelets present the advantage of square (or cubic) support, which makes easy the effective implementation of an automatic evolution of wavelet coefficients, when solving PDE problems (see for instance [5,21]). Moreover, in the context of turbulence, the (divergence-free!) flow is homogeneous: in this context, isotropic wavelet bases are more adapted to the structures of the flow, and adaptive schemes have been implemented [12].

Consequently we will construct new isotropic and quasi-isotropic divergence-free and curl-free wavelets, by considering anisotropic wavelets, whose parameters $\mathbf{j}$ verify $\max(\mathbf{j}) - \min(\mathbf{j}) \leqslant m$ with $m = 0, 1, 2$. We will then modify the div-free and curl-free wavelet transforms of Section 1.3, and establish a convergence theorem for the Helmholtz algorithm when $m \neq 0$.

This newer isotropic wavelet decomposition includes the older decomposition originally designed by Lemarié-Rieusset [16] and used by Urban [26]. It presents the advantage to avoid the arbitrary choice of an index i which plays the rôle of pivotal element to form the divergence-free wavelet basis. We will construct $(2^n - 1)n$ generating functions instead of the previous $(2^n - 1)(n - 1)$, to form a divergence-free basis in dimension n. The price to pay for this modification is that our divergence-free wavelets will form a redundant set. But we will take advantage of this redundancy for adding a useful linear combination of wavelet coefficients. This construction leads to a clearer understanding of the divergence-free wavelet transform in the isotropic case.

3.1. Generalized divergence-free and curl-free wavelets

3.1.1. Divergence-free wavelets

In the following, we will define generalized quasi-isotropic divergence-free wavelets by considering two kinds of divergence-free wavelets, with limitations on the scale parameter $\mathbf{j}$. Let $m \geqslant 0$ be given, we will only consider scale indices $\mathbf{j} = (j_1, j_2, \dots, j_n)$ such that $\max(j_1, j_2, \dots, j_n) - \min(j_1, j_2, \dots, j_n) \leqslant m$. Then the following functions form a frame of $\mathbf{H}_{\mathrm{div}\,0}(\mathbb{R}^n)$:

- usual anisotropic divergence-free wavelets $\Psi^{\mathrm{div}\,i}_{\mathbf{j},\mathbf{k}}$ with $1 \leqslant i \leqslant n$ as in Section 1.3,
- modified isotropic divergence-free vector wavelets $\Psi^{\mathrm{div}\,i}_{\varepsilon\mathbf{j},\mathbf{k}}$, with $\varepsilon \in \{0,1\}^n \setminus \{(0,\dots,0)\}$, $1 \leqslant i \leqslant n$, and with components of the type $\eta^{(\varepsilon_1)}_{j_1,k_1} \dots \eta^{(\varepsilon_n)}_{j_n,k_n}$, with $\eta^{(1)} = \psi$, $\eta^{(0)} = \varphi$, and $j_\ell = \max(j_1, j_2, \dots, j_n) - m$ if $\varepsilon_\ell = 0$.

To construct these last functions, we will introduce linear combinations of quasi-isotropic wavelets which are a mix of isotropic and anisotropic wavelets:

$$\Psi^i_{\varepsilon\mathbf{j},\mathbf{k}}(x_1,\dots,x_n) = \left| \begin{array}{l} 0 \\ \vdots \\ \eta_0^{(\varepsilon_1)}(2^{j_1}x_1 - k_1)\dots\eta_1^{(\varepsilon_i)}(2^{j_i}x_i - k_i)\dots\eta_0^{(\varepsilon_n)}(2^{j_n}x_n - k_n) \\ \vdots \\ 0 \end{array} \right. ,$$

where $\eta_\ell^{(\varepsilon_i)} = \begin{cases} \psi_\ell & \text{if } \varepsilon_i = 1, \\ \varphi_\ell & \text{if } \varepsilon_i = 0, \end{cases} \quad \ell = 0, 1.$

Taking into account the differentiation relations of Proposition 1.1, we have:

$$\big(\eta_1^{(\varepsilon_i)}\big)'(x) = 4^{\varepsilon_i}\big(\eta_0^{(\varepsilon_i)}(x) - (1-\varepsilon_i)\eta_0^{(\varepsilon_i)}(x-1)\big).$$

The set $\{\Psi^i_{\varepsilon\mathbf{j},\mathbf{k}}\colon\ 1 \leqslant i \leqslant n,\ \mathbf{j},\mathbf{k} \in \mathbb{Z}^n,\ \varepsilon \in \{0,1\}^n \setminus \{(0,\dots,0)\},\ \max(j_1, j_2, \dots, j_n) - \min(j_1, j_2, \dots, j_n) \leqslant m,\ \varepsilon_\ell = 0 \Rightarrow j_\ell = \max(j_1, j_2, \dots, j_n) - m\}$ forms a Riesz basis of $(L^2(\mathbb{R}^n))^n$.

We will now construct the n-dimensional quasi-isotropic divergence-free wavelets.

Definition 3.1. For $1 \leqslant i \leqslant n$, we define quasi-isotropic divergence-free wavelets by:

$$\begin{aligned} &\Psi^{\mathrm{div}\,i}_{\varepsilon\mathbf{j},\mathbf{k}}(x_1,\dots,x_n) \\ &= \left| \begin{array}{l} -2^{j_i+j_1}\varepsilon_1\eta_1^{(\varepsilon_1)}(2^{j_1}x_1-k_1)\dots(\eta_0^{(\varepsilon_i)}(2^{j_i}x_i-k_i)-(1-\varepsilon_i)\eta_0^{(\varepsilon_i)}(2^{j_i}x_i-k_i-1))\dots\eta_0^{(\varepsilon_n)}(2^{j_n}x_n-k_n) \\ \vdots \\ 4^{1-\varepsilon_i}(\sum_{\ell\neq i,\,\varepsilon_\ell=1} 2^{2j_\ell})\eta_0^{(\varepsilon_1)}(2^{j_1}x_1-k_1)\dots\eta_1^{(\varepsilon_i)}(2^{j_i}x_i-k_i)\dots\eta_0^{(\varepsilon_n)}(2^{j_n}x_n-k_n) \\ \vdots \\ -2^{j_i+j_n}\varepsilon_n\eta_0^{(\varepsilon_1)}(2^{j_1}x_1-k_1)\dots(\eta_0^{(\varepsilon_i)}(2^{j_i}x_i-k_i)-(1-\varepsilon_i)\eta_0^{(\varepsilon_i)}(2^{j_i}x_i-k_i-1))\dots\eta_1^{(\varepsilon_n)}(2^{j_n}x_n-k_n) \end{array} \right. . \end{aligned}$$

The complementary wavelet is given by:

$$\Psi^{\mathfrak{N}}_{\varepsilon\mathbf{j},\mathbf{k}}(x_1,\dots,x_n) = \left| \begin{array}{l} 2^{j_1}\varepsilon_1\eta_1^{(\varepsilon_1)}(2^{j_1}x_1-k_1)\dots\eta_0^{(\varepsilon_i)}(2^{j_i}x_i-k_i)\dots\eta_0^{(\varepsilon_n)}(2^{j_n}x_n-k_n) \\ \vdots \\ 2^{j_n}\varepsilon_n\eta_0^{(\varepsilon_1)}(2^{j_1}x_1-k_1)\dots\eta_0^{(\varepsilon_i)}(2^{j_i}x_i-k_i)\dots\eta_1^{(\varepsilon_n)}(2^{j_n}x_n-k_n) \end{array} \right. .$$

Remark that the case $m = 0$ corresponds to linear combinations of the isotropic divergence-free wavelets proposed by P.G. Lemarié-Rieusset and K. Urban [16,26]. Note also that $\Psi^{\mathfrak{N}}_{\varepsilon\mathbf{j},\mathbf{k}}$ is no more orthogonal to $\Psi^{\mathrm{div}\,i}_{\varepsilon\mathbf{j},\mathbf{k}}$, except if $\varepsilon_i = 1$.

3.1.2. Divergence-free fast transforms

If we denote by $(d_{i,\varepsilon\mathbf{j},\mathbf{k}})$ the wavelet coefficients of a function $\mathbf{u}$ in the basis $\{\Psi^i_{\varepsilon\mathbf{j},\mathbf{k}}\}$, then we obtain the divergence-free wavelet and complementary wavelet coefficients by solving the following system for fixed $\mathbf{j}, \mathbf{k}, \varepsilon$:

$$M_{\mathrm{div}} \begin{bmatrix} d_{\mathrm{div}\,1,\varepsilon\mathbf{j},\mathbf{k}} \\ \vdots \\ d_{\mathrm{div}\,n,\varepsilon\mathbf{j},\mathbf{k}} \\ d_{\mathfrak{N}\,\varepsilon\mathbf{j},\mathbf{k}} \end{bmatrix} + \sum_{i,\,\varepsilon_i=0} M^{(i)}_{\mathrm{div}} \begin{bmatrix} d_{\mathrm{div}\,1,\varepsilon\mathbf{j},\mathbf{k}-e_i} \\ \vdots \\ d_{\mathrm{div}\,n,\varepsilon\mathbf{j},\mathbf{k}-e_i} \\ d_{\mathfrak{N}\,\varepsilon\mathbf{j},\mathbf{k}-e_i} \end{bmatrix} = \begin{bmatrix} d_{1,\varepsilon\mathbf{j},\mathbf{k}} \\ \vdots \\ d_{n,\varepsilon\mathbf{j},\mathbf{k}} \\ 0 \end{bmatrix} \tag{3.1}$$

with $(e_i)_{1\leqslant i\leqslant n}$ the canonical basis of $\mathbb{R}^n$. We introduce the notations $\omega_i = 2^{j_i}$ and $|\varepsilon\omega|^2 = \sum_{i,\,\varepsilon_i=1}\omega_i^2$, and the normalization of the wavelets:

$$\Psi^{\mathrm{div}\,i}_{\varepsilon\mathbf{j},\mathbf{k}} \mapsto \frac{1}{|\varepsilon\omega|^2}\Psi^{\mathrm{div}\,i}_{\varepsilon\mathbf{j},\mathbf{k}}, \qquad \Psi^{\mathfrak{N}}_{\varepsilon\mathbf{j},\mathbf{k}} \mapsto \frac{1}{|\varepsilon\omega|}\Psi^{\mathfrak{N}}_{\varepsilon\mathbf{j},\mathbf{k}}.$$

Then the expressions of M_{div} and $M^{(i)}_{\mathrm{div}}$ are chosen as follows (the last line represents an arbitrary linear combination of the divergence-free wavelet coefficients):

$$M_{\mathrm{div}} = \begin{bmatrix} 4^{1-\varepsilon_1}(1-\varepsilon_1\frac{\omega_1^2}{|\varepsilon\omega|^2}) & -\varepsilon_1\frac{\omega_2\omega_1}{|\varepsilon\omega|^2} & \dots & -\varepsilon_1\frac{\omega_n\omega_1}{|\varepsilon\omega|^2} & \varepsilon_1\frac{\omega_1}{|\varepsilon\omega|} \\ -\varepsilon_2\frac{\omega_1\omega_2}{|\varepsilon\omega|^2} & 4^{1-\varepsilon_2}(1-\varepsilon_2\frac{\omega_2^2}{|\varepsilon\omega|^2}) & \ddots & -\varepsilon_2\frac{\omega_n\omega_2}{|\varepsilon\omega|^2} & \varepsilon_2\frac{\omega_2}{|\varepsilon\omega|} \\ \vdots & \vdots & \ddots & \vdots & \vdots \\ -\varepsilon_n\frac{\omega_1\omega_n}{|\varepsilon\omega|^2} & -\varepsilon_n\frac{\omega_2\omega_n}{|\varepsilon\omega|^2} & \dots & 4^{1-\varepsilon_n}(1-\varepsilon_n\frac{\omega_n^2}{|\varepsilon\omega|^2}) & \varepsilon_n\frac{\omega_n}{|\varepsilon\omega|} \\ \varepsilon_1\frac{\omega_1}{|\varepsilon\omega|} & \varepsilon_2\frac{\omega_2}{|\varepsilon\omega|} & \dots & \varepsilon_n\frac{\omega_n}{|\varepsilon\omega|} & 0 \end{bmatrix} \tag{3.2}$$

and

$$M^{(i)}_{\mathrm{div}} = \begin{bmatrix} 0 & \dots 0 & \varepsilon_1\frac{\omega_i\omega_1}{|\varepsilon\omega|^2} & 0 & \dots & 0 \\ \vdots & \vdots & \vdots & \vdots & \vdots & \vdots \\ 0 & \dots 0 & \varepsilon_n\frac{\omega_i\omega_n}{|\varepsilon\omega|^2} & 0 & \dots & 0 \\ 0 & \dots 0 & 0 & 0 & \dots & 0 \end{bmatrix} \tag{3.3}$$

where only the column number i of $M^{(i)}_{\mathrm{div}}$ is different from zero.

One can notice that for all indices i such that $\varepsilon_i = 0$,

$$d_{\mathrm{div}\,i,\varepsilon\mathbf{j},\mathbf{k}} = \frac{1}{4}d_{i,\varepsilon\mathbf{j},\mathbf{k}}.$$

Then system (3.1) is equivalent to:

$$M_{\mathrm{div}}\begin{bmatrix} \varepsilon_1 d_{\mathrm{div}\,1,\varepsilon\mathbf{j},\mathbf{k}} \\ \vdots \\ \varepsilon_n d_{\mathrm{div}\,n,\varepsilon\mathbf{j},\mathbf{k}} \\ d_{\mathfrak{N}\,\varepsilon\mathbf{j},\mathbf{k}} \end{bmatrix} = \begin{bmatrix} d_{1,\varepsilon\mathbf{j},\mathbf{k}} \\ \vdots \\ d_{n,\varepsilon\mathbf{j},\mathbf{k}} \\ 0 \end{bmatrix} - \frac{1}{4}M_{\mathrm{div}}\begin{bmatrix} (1-\varepsilon_1)d_{1,\varepsilon\mathbf{j},\mathbf{k}} \\ \vdots \\ (1-\varepsilon_n)d_{n,\varepsilon\mathbf{j},\mathbf{k}} \\ 0 \end{bmatrix} - \frac{1}{4}\sum_{i,\,\varepsilon_i=0} M^{(i)}_{\mathrm{div}}\begin{bmatrix} d_{1,\varepsilon\mathbf{j},\mathbf{k}-e_i} \\ \vdots \\ d_{n,\varepsilon\mathbf{j},\mathbf{k}-e_i} \\ 0 \end{bmatrix}.$$

To solve (3.1), we multiply the above system by the matrix:

$$\begin{bmatrix} (1-\frac{\varepsilon_1\omega_1^2}{|\varepsilon\omega|^2}) & -\varepsilon_2\varepsilon_1\frac{\omega_2\omega_1}{|\varepsilon\omega|^2} & \dots & -\varepsilon_n\varepsilon_1\frac{\omega_n\omega_1}{|\varepsilon\omega|^2} & \varepsilon_1\frac{\omega_1}{|\varepsilon\omega|} \\ -\varepsilon_1\varepsilon_2\frac{\omega_1\omega_2}{|\varepsilon\omega|^2} & (1-\frac{\varepsilon_2\omega_2^2}{|\varepsilon\omega|^2}) & \ddots & -\varepsilon_n\varepsilon_2\frac{\omega_n\omega_2}{|\varepsilon\omega|^2} & \varepsilon_2\frac{\omega_2}{|\varepsilon\omega|} \\ \vdots & \vdots & \ddots & \vdots & \vdots \\ -\varepsilon_1\varepsilon_n\frac{\omega_1\omega_n}{|\varepsilon\omega|^2} & -\varepsilon_2\varepsilon_n\frac{\omega_2\omega_n}{|\varepsilon\omega|^2} & \dots & (1-\frac{\varepsilon_n\omega_n^2}{|\varepsilon\omega|^2}) & \varepsilon_n\frac{\omega_n}{|\varepsilon\omega|} \\ \varepsilon_1\frac{\omega_1}{|\varepsilon\omega|} & \varepsilon_2\frac{\omega_2}{|\varepsilon\omega|} & \dots & \varepsilon_n\frac{\omega_n}{|\varepsilon\omega|} & 0 \end{bmatrix} \tag{3.4}$$

and we find that for indices i such that $\varepsilon_i = 1$,

$$d_{\mathrm{div}\,i,\varepsilon\mathbf{j},\mathbf{k}} = d_{i,\varepsilon\mathbf{j},\mathbf{k}} - \frac{\omega_i}{|\varepsilon\omega|^2}\sum_{\ell=1}^{n}\varepsilon_\ell\omega_\ell d_{\ell,\varepsilon\mathbf{j},\mathbf{k}}$$

and

$$d_{\mathfrak{N}\,\varepsilon\mathbf{j},\mathbf{k}} = \sum_{i,\,\varepsilon_i=1}\frac{\omega_i}{|\varepsilon\omega|}d_{i,\varepsilon\mathbf{j},\mathbf{k}} + \sum_{i,\,\varepsilon_i=0}\frac{\omega_i}{4|\varepsilon\omega|}(d_{i,\varepsilon\mathbf{j},\mathbf{k}} - d_{i,\varepsilon\mathbf{j},\mathbf{k}-e_i}).$$

We proceed similarly as in Section 2.3 when we establish (2.20) to derive the Fourier transform of $\mathrm{Q}_{\mathfrak{N}}\mathbf{u}_{\varepsilon\mathbf{j}}$:

$$\widehat{\mathrm{Q}_{\mathfrak{N}}\mathbf{u}_{\varepsilon\mathbf{j}}} = \frac{1}{|\varepsilon\omega|^2}\begin{bmatrix} \varepsilon_1\frac{\omega_1^2}{\xi_1} \\ \vdots \\ \varepsilon_n\frac{\omega_n^2}{\xi_n}\end{bmatrix} \times [\xi_1 \dots \xi_n]\widehat{\mathbf{u}_{\varepsilon\mathbf{j}}}$$

which will be used in the next section.

3.1.3. Curl-free quasi-isotropic wavelets

The n-dimensional quasi-isotropic curl-free wavelets are defined by:

$$\Psi^{\mathrm{curl}}_{\varepsilon\mathbf{j},\mathbf{k}}(x_1,\dots,x_n) = \left| \begin{array}{l} 2^{j_1}\cdot 4^{\varepsilon_1-1}(\eta_0^{(\varepsilon_1)}(2^{j_1}x_1-k_1)-(1-\varepsilon_1)\eta_0^{(\varepsilon_1)}(2^{j_1}x_1-k_1-1))\dots\eta_1^{(\varepsilon_i)}(2^{j_i}x_i-k_i)\dots\eta_1^{(\varepsilon_n)}(2^{j_n}x_n-k_n) \\ \vdots \\ 2^{j_i}\cdot 4^{\varepsilon_i-1}\eta_1^{(\varepsilon_1)}(2^{j_1}x_1-k_1)\dots(\eta_0^{(\varepsilon_i)}(2^{j_i}x_i-k_i)-(1-\varepsilon_i)\eta_0^{(\varepsilon_i)}(2^{j_i}x_i-k_i-1))\dots\eta_1^{(\varepsilon_n)}(2^{j_n}x_n-k_n) \\ \vdots \\ 2^{j_n}\cdot 4^{\varepsilon_n-1}\eta_1^{(\varepsilon_1)}(2^{j_1}x_1-k_1)\dots\eta_1^{(\varepsilon_i)}(2^{j_i}x_i-k_i)\dots(\eta_0^{(\varepsilon_n)}(2^{j_n}x_n-k_n)-(1-\varepsilon_n)\eta_0^{(\varepsilon_n)}(2^{j_n}x_n-k_n-1)) \end{array}\right.$$

and the complementary wavelets are defined for $1 \leqslant i \leqslant n$ by:

$$\Psi^{\mathcal{N}\,i}_{\varepsilon\mathbf{j},\mathbf{k}}(x_1,\dots,x_n) = \left| \begin{array}{l} -2^{j_i+j_1}\varepsilon_i\varepsilon_1\eta_0^{(\varepsilon_1)}(2^{j_1}x_1-k_1)\dots\eta_1^{(\varepsilon_i)}(2^{j_i}x_i-k_i)\dots\eta_1^{(\varepsilon_n)}(2^{j_n}x_n-k_n) \\ \vdots \\ (\sum_{\ell\neq i,\,\varepsilon_\ell=1}2^{2j_\ell})\eta_1^{(\varepsilon_1)}(2^{j_1}x_1-k_1)\dots\eta_0^{(\varepsilon_i)}(2^{j_i}x_i-k_i)\dots\eta_1^{(\varepsilon_n)}(2^{j_n}x_n-k_n)\ . \\ \vdots \\ -2^{j_i+j_n}\varepsilon_i\varepsilon_n\eta_1^{(\varepsilon_1)}(2^{j_1}x_1-k_1)\dots\eta_1^{(\varepsilon_i)}(2^{j_i}x_i-k_i)\dots\eta_0^{(\varepsilon_n)}(2^{j_n}x_n-k_n) \end{array}\right.$$

After renormalization of the wavelets ($\Psi^{\mathrm{curl}}_{\varepsilon\mathbf{j},\mathbf{k}}$ is divided by $|\varepsilon\omega|$ and $\Psi^{\mathcal{N}\,i}_{\varepsilon\mathbf{j},\mathbf{k}}$ by $|\varepsilon\omega|^2$), the wavelet coefficients verify, for fixed $\mathbf{j}$, $\mathbf{k}$, ε:

$$M_{\mathrm{curl}}\begin{bmatrix} d_{\mathcal{N}\,1,\varepsilon\mathbf{j},\mathbf{k}} \\ \vdots \\ d_{\mathcal{N}\,n,\varepsilon\mathbf{j},\mathbf{k}} \\ d_{\mathrm{curl}\,\varepsilon\mathbf{j},\mathbf{k}}\end{bmatrix} + \sum_{i,\,\varepsilon_i=0} M^{(i)}_{\mathrm{curl}}\begin{bmatrix} d_{\mathcal{N}\,1,\varepsilon\mathbf{j},\mathbf{k}-e_i} \\ \vdots \\ d_{\mathcal{N}\,n,\varepsilon\mathbf{j},\mathbf{k}-e_i} \\ d_{\mathrm{curl}\,\varepsilon\mathbf{j},\mathbf{k}-e_i}\end{bmatrix} = \begin{bmatrix} d_{1,\varepsilon\mathbf{j},\mathbf{k}} \\ \vdots \\ d_{n,\varepsilon\mathbf{j},\mathbf{k}} \\ 0\end{bmatrix} \tag{3.5}$$

where the matrices M_{curl} and $M^{(i)}_{\mathrm{curl}}$ for $1 \leqslant i \leqslant n$ are given by:

$$M_{\mathrm{curl}} = \begin{bmatrix} (1-\varepsilon_1\frac{\omega_1^2}{|\varepsilon\omega|^2}) & -\varepsilon_2\varepsilon_1\frac{\omega_2\omega_1}{|\varepsilon\omega|^2} & \dots & -\varepsilon_n\varepsilon_1\frac{\omega_n\omega_1}{|\varepsilon\omega|^2} & 4^{\varepsilon_1-1}\frac{\omega_1}{|\varepsilon\omega|} \\ -\varepsilon_1\varepsilon_2\frac{\omega_1\omega_2}{|\varepsilon\omega|^2} & (1-\varepsilon_2\frac{\omega_2^2}{|\varepsilon\omega|^2}) & \ddots & -\varepsilon_n\varepsilon_2\frac{\omega_n\omega_2}{|\varepsilon\omega|^2} & 4^{\varepsilon_2-1}\frac{\omega_2}{|\varepsilon\omega|} \\ \vdots & \vdots & \ddots & \vdots & \vdots \\ -\varepsilon_1\varepsilon_n\frac{\omega_1\omega_n}{|\varepsilon\omega|^2} & -\varepsilon_2\varepsilon_n\frac{\omega_2\omega_n}{|\varepsilon\omega|^2} & \dots & (1-\varepsilon_n\frac{\omega_n^2}{|\varepsilon\omega|^2}) & 4^{\varepsilon_n-1}\frac{\omega_n}{|\varepsilon\omega|} \\ \varepsilon_1\frac{\omega_1}{|\varepsilon\omega|} & \varepsilon_2\frac{\omega_2}{|\varepsilon\omega|} & \dots & \varepsilon_n\frac{\omega_n}{|\varepsilon\omega|} & 0 \end{bmatrix} \tag{3.6}$$

and

$$M^{(i)}_{\mathrm{curl}} = \begin{bmatrix} 0 & \dots & 0 & 0 \\ \vdots & \vdots & \vdots & \vdots \\ 0 & \dots & 0 & 0 \\ 0 & \dots & 0 & -\frac{\omega_i}{4|\varepsilon\omega|} \\ 0 & \dots & 0 & 0 \\ \vdots & \vdots & \vdots & \vdots \\ 0 & \dots & 0 & 0 \end{bmatrix} \tag{3.7}$$

where only the line number i of $M^{(i)}_{\mathrm{curl}}$ is non-zero.

To solve the system of Eqs. (3.5), we multiply it by the matrix (3.4) and we find:

$$d_{\mathrm{curl}\,\varepsilon\mathbf{j},\mathbf{k}} = \sum_{i=1}^{n} \varepsilon_i \frac{\omega_i}{|\varepsilon\omega|} d_{i,\varepsilon\mathbf{j},\mathbf{k}}$$

which means that the Fourier transform of $\mathrm{P}_{\mathcal{N}}\mathbf{u}_{\varepsilon\mathbf{j}}$ satisfies:

$$\widehat{\mathrm{P}_{\mathcal{N}}\mathbf{u}_{\varepsilon\mathbf{j}}} = \left(Id - \frac{1}{|\varepsilon\omega|^2} \begin{bmatrix} \xi_1 \\ \vdots \\ \xi_n \end{bmatrix} \times \left[\varepsilon_1 \frac{\omega_1^2}{\xi_1} \ldots \varepsilon_n \frac{\omega_n^2}{\xi_n} \right] \right) \widehat{\mathbf{u}_{\varepsilon\mathbf{j}}}.$$

The expression of the wavelet coefficients $d_{\mathcal{N}\,i,\varepsilon\mathbf{j},\mathbf{k}}$ is, for $\varepsilon_i = 1$:

$$d_{\mathcal{N}\,i,\varepsilon\mathbf{j},\mathbf{k}} = d_{i,\varepsilon\mathbf{j},\mathbf{k}} - \frac{\omega_i}{|\varepsilon\omega|^2} \sum_{\ell=1}^{n} \varepsilon_\ell \omega_\ell d_{\ell,\varepsilon\mathbf{j},\mathbf{k}}$$

and for $\varepsilon_i = 0$:

$$d_{\mathcal{N}\,i,\varepsilon\mathbf{j},\mathbf{k}} = d_{i,\varepsilon\mathbf{j},\mathbf{k}} + \frac{\omega_i}{4|\varepsilon\omega|^2} \sum_{\ell=1}^{n} \varepsilon_\ell \omega_\ell d_{\ell,\varepsilon\mathbf{j},\mathbf{k}-e_i}.$$

3.2. Convergence of the iterative Helmholtz decomposition in the generalized case

Theorem 3.1. *In dimension n, the wavelet Helmholtz algorithm* (2.6) *defined in Section* 2.1 *converges using Shannon wavelets, if*

$$m > \frac{1}{2\ln 2} \ln \frac{16n}{7}$$

in the construction of the generalized divergence-free and curl-free wavelets (*cf. Section* 3.1).

Proof. Assume that we are using Shannon wavelets, each level of the wavelet decomposition (indexed by $\mathbf{j} \in \mathbb{Z}^n$ with $\max(\mathbf{j}) - \min(\mathbf{j}) \leqslant m$ and by $\varepsilon \in \{0,1\}^n \setminus \{(0,\ldots,0)\}$) evolves independently during the wavelet Helmholtz decomposition algorithm (2.6). Hence:

$$\widehat{\mathbf{u}_{\varepsilon\mathbf{j}}^{p+1}} = A\widehat{\mathbf{u}_{\varepsilon\mathbf{j}}^{p}}$$

with

$$A = \left(Id - \frac{1}{|\varepsilon\omega|^2} \begin{bmatrix} \xi_1 \\ \vdots \\ \xi_n \end{bmatrix} \times \left[\varepsilon_1 \frac{\omega_1^2}{\xi_1} \ldots \varepsilon_n \frac{\omega_n^2}{\xi_n} \right] \right) \times \frac{1}{|\varepsilon\omega|^2} \begin{bmatrix} \varepsilon_1 \frac{\omega_1^2}{\xi_1} \\ \vdots \\ \varepsilon_n \frac{\omega_n^2}{\xi_n} \end{bmatrix} \times [\xi_1 \ldots \xi_n].$$

This matrix is of rank one and has a single non-zero eigenvalue λ, equal to the trace of A:

$$\lambda = 1 - \left(\sum_{i=1}^{n} \frac{\xi_i^2}{|\varepsilon\omega|^4} \right) \left(\sum_{i=1}^{n} \frac{\varepsilon_i \omega_i^4}{\xi_i^2} \right)$$

i.e., with $\zeta_i = \frac{\xi_i}{\omega_i} \in \pm[\pi, 2\pi]$ if $\varepsilon_i = 1$, $\zeta_i \in [-\pi, \pi]$ if $\varepsilon_i = 0$,

$$\lambda = 1 - \left(\sum_{i=1}^{n} \frac{\omega_i^2}{|\varepsilon\omega|^2} \zeta_i^2 \right) \left(\sum_{i=1}^{n} \frac{\omega_i^2}{|\varepsilon\omega|^2} \varepsilon_i \zeta_i^{-2} \right)$$

which can be rewritten, if we distinguish the case $\varepsilon_i = 1$ and $\varepsilon_i = 0$ in the first sum:

$$\lambda = 1 - \left(\sum_{i=1}^{n} \frac{\varepsilon_i \omega_i^2}{|\varepsilon\omega|^2} \zeta_i^2 \right) \left(\sum_{i=1}^{n} \frac{\varepsilon_i \omega_i^2}{|\varepsilon\omega|^2} \zeta_i^{-2} \right) - \left(\sum_{i=1}^{n} (1-\varepsilon_i) \frac{\omega_i^2}{|\varepsilon\omega|^2} \zeta_i^2 \right) \left(\sum_{i=1}^{n} \frac{\omega_i^2}{|\varepsilon\omega|^2} \varepsilon_i \zeta_i^{-2} \right).$$

For the first term, we use the Kantorovich inequality (2.23). We denote by μ the second term:

$$\mu = \left(\sum_{i=1}^{n} (1-\varepsilon_i) \frac{\omega_i^2}{|\varepsilon\omega|^2} \zeta_i^2 \right) \left(\sum_{i=1}^{n} \frac{\omega_i^2}{|\varepsilon\omega|^2} \varepsilon_i \zeta_i^{-2} \right) \geqslant 0,$$

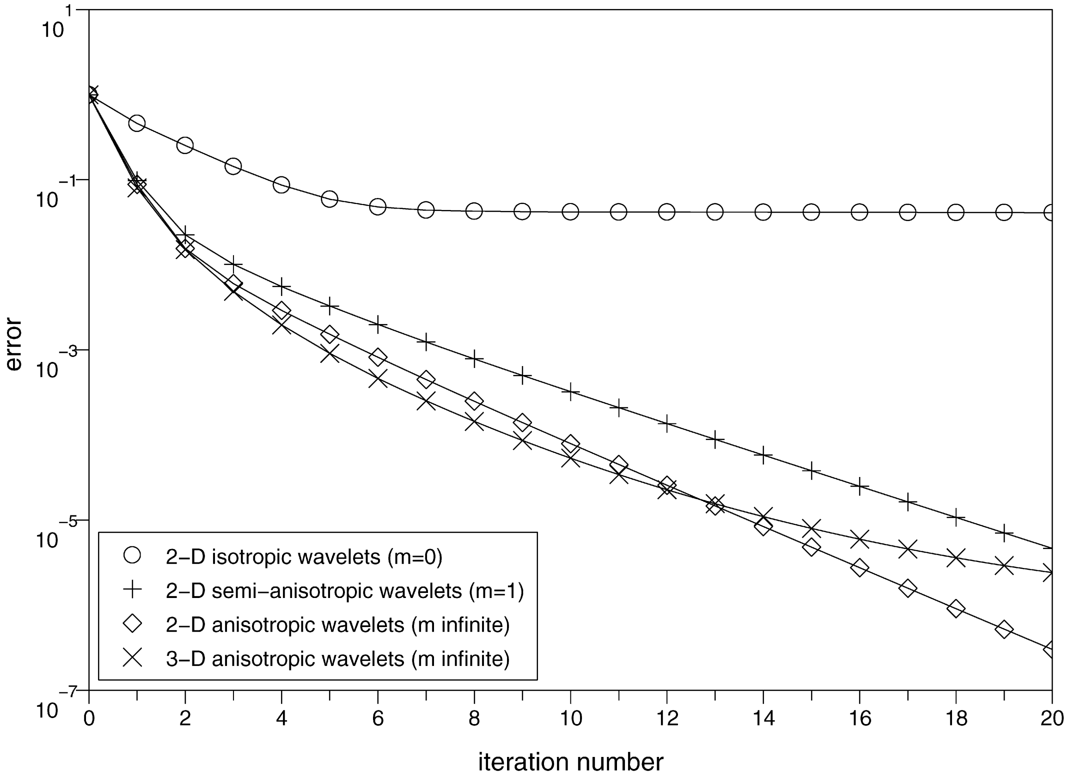

Fig. 1. Convergence profiles of the wavelet Helmholtz algorithm with spline wavelets of different degrees of anisotropy (norm of the residue in terms of number of iterations).

then

$$-\frac{9}{16}-\mu \leqslant \lambda \leqslant -\mu. \tag{3.8}$$

As for i s.t. $\varepsilon_i=0$, $\omega_i \leqslant 2^{-m}|\varepsilon\omega|$ and $\zeta_i^2 \leqslant \pi^2$, and for i s.t. $\varepsilon_i=1$, $\zeta_i^{-2} \leqslant \pi^{-2}$, μ is bounded by

$$\mu \leqslant \sum_{i=1}^{n}(1-\varepsilon_i)2^{-2m}\pi^2 \sum_{i=1}^{n}\frac{\varepsilon_i\omega_i^2}{|\varepsilon\omega|^2}\pi^{-2} \leqslant 2^{-2m}n.$$

Since according to (3.8), a sufficient condition for the convergence is $\mu < \frac{7}{16}$, this condition will be satisfied provided that

$$m > \frac{1}{2\ln 2}\ln\frac{16n}{7}.$$

Consequently the number m of additional wavelet transforms we have to apply after an isotropic wavelet transform, is not excessive. □

Remark 3.1. Again, as it was proposed in Section 2.3, we may introduce a parameter $b>0$ in the algorithm (2.6): $\mathbf{u}^{p+1} = \mathbf{u}^p - \mathbf{u}_{\mathrm{div}}^p - b\mathbf{u}_{\mathrm{curl}}^p$. Then, according to the previous study, the following bounds hold for the eigenvalue $\lambda(\xi)$, using Shannon wavelets:

$$1-b\left(\frac{25}{16}+2^{-2m}n\right) \leqslant \lambda(\xi) \leqslant 1-b.$$

The algorithm converges for b sufficiently small. In practice, with spline wavelets, whatever the value of b, the algorithm (2.6) does not converge for isotropic wavelets ($m=0$) and presents the same profile as in Fig. 1.

4. Numerical experiments

The wavelet Helmholtz algorithm was applied to non divergence-free periodic vector fields on the cube $[0,1]^n$ ($n=2,3$), in order to observe the convergence rate of the iterative algorithm. We will compare the convergence according to the isotropic or anisotropic nature of the divergence-free wavelets and for different spline wavelets.

Table 1
Convergence rates observed for various spline wavelets ψ_1 and duals ψ_1^*

Number of zero moments for ψ_1	Number of zero moments for ψ_1^*		
	2	3	4
1	1.24	0.56	0.64
2	0.57	0.56	0.35
3	0.59	0.35	0.42
4	0.44	0.42	
5	0.45		

Ref. [8] provides technical explanations for the implementation of the method. We have already tested in [8] the convergence of our iterative algorithm, using spline wavelets of different orders, successfully applied to a large class of two and three-dimensional fields. The observed convergence rates were about 0.5 (see also Fig. 1).

4.1. Comparison isotropic/anisotropic wavelets

For this comparison, we have used spline wavelets: the functions (φ_0, ψ_0) are splines of order two (i.e. piecewise polynomials of degree one), and the functions (φ_1, ψ_1) are splines of order three (i.e. piecewise polynomials of degree two). We have compared the convergence rates obtained with several families of generalized divergence-free and curl-free wavelets. We have applied the wavelet Helmholtz algorithm to the 2D vector field

$$\mathbf{u} = \left| \begin{array}{l} -\sin(2\pi x)\cos(2\pi y) \\ -\cos(2\pi x)\sin(2\pi y) - 2\sin(2\pi x)\cos(2\pi y) \end{array} \right.$$

discretized on a 256^2 point grid, and to the 3D vector field:

$$\mathbf{u} = \left| \begin{array}{l} -\sin(2\pi x)\cos(2\pi y)\cos(2\pi z) + \sin(2\pi x)\cos(2\pi y) - \sin(2\pi x)\cos(2\pi z) \\ -\cos(2\pi x)\sin(2\pi y)\cos(2\pi z) + \sin(2\pi y)\cos(2\pi z) - \cos(2\pi x)\sin(2\pi y) \\ -\cos(2\pi x)\cos(2\pi y)\sin(2\pi z) + \cos(2\pi x)\sin(2\pi z) - \cos(2\pi y)\sin(2\pi z) \end{array} \right.$$

discretized on a point 32^3 grid. Fig. 1 shows the evolution of the residue $\|\mathbf{u}^p\|_{L^2}$ in terms of the number of iterations p. In Fig. 1 we have used four different wavelet bases:

- two-dimensional isotropic (i.e. $m = 0$) functions, and this choice leads to the non-convergence of the algorithm,
- two-dimensional anisotropic (i.e. $m = +\infty$) functions,
- two-dimensional quasi-isotropic (with $m = 1$) functions, and
- three-dimensional anisotropic functions.

These experiments clearly show that isotropic functions are not well suited to be used in our wavelet Helmholtz algorithm. In all other cases (anisotropic and quasi-isotropic), the algorithm converges. At the end of the execution, the accuracy depends on the spline order of the wavelets. The change of behavior for the three-dimensional case in the last steps is related to the spline interpolation, which has been optimized in the code for dimension two (cf. [8]) but not for dimension three.

4.2. Link between order of the wavelet basis and convergence rate

We have also tested the wavelet Helmholtz algorithm on a 2D periodic function discretized on a 256×256 grid, for different splines. If ψ_1 is a spline of order n (which is equivalent to ψ_1^* has n vanishing moments) with m vanishing moments, then ψ_0 is a spline function of order $n-1$ with $m+1$ vanishing moments. We have used linear, quadratic and cubic splines for ψ_1, in order to observe the effects of the basis order on the convergence rate. The results are presented in Table 1. The convergence rate has been measured in the linear part of the slope which can be observed in Fig. 1.

Increasing the number of vanishing moments for the wavelet or for its dual improves the convergence rate. The best results obtained in the cases $(1,3)$, $(2,2)$, and $(2,4)$, $(3,3)$ and $(4,2)$ can be explained by the symmetry of the wavelets in these configurations. In the case $(1,2)$, the algorithm diverges.

4.3. Computational cost

The wavelet Helmholtz algorithm presented in this paper only uses fast wavelet transforms, at each iteration. The total computational cost can be compared with the cost of a Leray projection computed by fast Fourier transform.

In the Fourier case, the computation of the Leray projection in dimension n requires in each direction a FFT followed by a n^2-matrix–vector multiplication (see (1.11)) at each wavenumber. Since in practice $n \ll N$, where N is the number of grid-points, the total computational cost of the Leray projection scale as $0(nN\log_2 N)$ operations.

On the other hand, the wavelet Helmholtz algorithm requires at each iteration, n fast wavelet transforms, followed by a n^2-matrix–vector multiplication (see (1.13)) for each index $(\mathbf{j}, \mathbf{k})$. Since a fast wavelet transform requires $O(nhN)$ operations (where h is the length of the wavelet filter), then each iteration of the wavelet Helmholtz algorithm needs $0(n^2 + hn)N$ operations. The total computational cost for our algorithm is about $0(n_{iter}nhN)$ (if $n < h$ which is usual), where n_{iter} is the number of iterations needed by the algorithm to converge. In our practical experiments, 20 iterations are sufficient to reach a relative error less than 10^{-7}. For a bidimensional vector field ($N = 1024^2$), using order 2 spline wavelets ($h = 4$), the computational cost of the wavelet Helmholtz decomposition is about 5-times less advantageous than a computation by FFT.

But one advantage of the wavelet Helmholtz algorithm is that it can be performed in adaptive situations, whereas the Fourier transform works only on regular grids. Another worthwhile situation is when the initial condition is close to the result, this is the case for instance in the simulation of incompressible Navier–Stokes equations [10]: at each time-step, the wavelet Helmholtz decomposition requires only 3 or 4 iterations to update the solution, which is comparable to computations performed by FFT.

5. Conclusion

In this article, we have constructed anisotropic divergence-free and curl-free wavelets in dimension n, by generalization of the constructions in 2D and 3D. To obtain small orthogonal systems for the computation of related coefficients, we have modified the original constructions of divergence-free wavelets (and thus curl-free wavelets) by analogy with the Leray projector written in Fourier domain. These new formulations have allowed us to define an iterative algorithm for the wavelet Helmholtz decomposition of any vector field, and we have proved its convergence in 2D for general wavelets and in nD for the particular case of Shannon wavelets. Moreover we have proved its convergence for quasi-isotropic wavelets. We have observed in numerical experiments that the convergence rate of the method depends on the number of vanishing moments of the wavelets and their duals, and also on the degree of anisotropy of the basis functions.

The interest of such wavelet Helmholtz decomposition is that it is localized in space contrarily to a decomposition computed by Fourier transform. This algorithm is well adapted for wavelet adaptive schemes, by using quasi-isotropic wavelets. This makes the method very attractive for large dimensional problems and it opens new prospects, for example for the direct numerical simulation of turbulence using divergence-free wavelet bases [6,8].

An important issue that must be addressed is the flexibility of the method: the method should be extended to bounded and non-periodic tensor-product domains, with physical boundary conditions, by using wavelets on the interval incorporating homogeneous boundary conditions, such as those in [20]. Indeed, the construction of a non-periodic divergence-free wavelet basis on the cube $[0, 1]^n$ has already been carried on by Lemarié-Rieusset and Jouini in [17]. This construction extends readily to curl-free wavelets, and to homogeneous boundary conditions. Work is in progress to implement these new wavelets and their related fast algorithms. Their practical use in a wavelet Helmholtz decomposition is underway and will be presented in a forthcoming paper.

Finally, these constructions and computational methods address the issue of numerical algorithms based on divergence-free wavelets for solving differential problems. The approach used in this article can be generalized to linear differential problems in order to provide original wavelet solvers (see [7]).

Acknowledgments

The authors would like to thank Kai Bittner, Nicholas Kevlahan and Karsten Urban for fruitful discussions. E.D. acknowledges support by E.U. project TODEQ (Operator Theory Methods for Differential Equations) contract No. MTKD-CT-2005-030042.

References

[1] K. Bittner, K. Urban, On interpolatory divergence-free wavelets, Math. Comp. 76 (2007) 903–929.
[2] A.J. Chorin, J.E. Marsden, A Mathematical Introduction to Fluid Mechanics, third ed., Springer, 1993.
[3] A. Cohen, I. Daubechies, J.C. Feauveau, Biorthogonal bases of compactly supported wavelets, Comm. Pure Appl. Math. 45 (1992) 485–560.
[4] A. Cohen, Numerical Analysis of Wavelet Methods, Stud. Math. Appl., Elsevier, Amsterdam, 2003.
[5] A. Cohen, W. Dahmen, R. De Vore, Adaptive wavelet techniques in numerical simulation, in: E. Stein, R. De Borst, T.J.R. Hughes (Eds.), Encyclopedia of Computational Mechanics, John Whiley & Sons, 2004.
[6] E. Deriaz, Ondelettes pour la simulation des écoulements fluides incompressibles en turbulence, PhD thesis in applied mathematics, INP Grenoble, March 2006 (in French).
[7] E. Deriaz, Shannon wavelet approximations of linear differential operators, Preprint IMPAN 676, January 2007.
[8] E. Deriaz, V. Perrier, Divergence-free and curl-free wavelets in 2D and 3D, application to turbulent flows, J. Turbul. 7 (3) (2006) 1–37.
[9] E. Deriaz, K. Bittner, V. Perrier, Décomposition de Helmholtz par ondelettes : convergence d'un algorithme itératif (Wavelet Helmholtz decomposition: Convergence of an iterative algorithm), ESAIM Proc. 18 (2007) 23–37 (in French).
[10] E. Deriaz, V. Perrier, Direct numerical simulation of turbulence using divergence-free wavelets, Preprint 684 of IMPAN, June 2007, http://www.impan.gov.pl/EN/Preprints/index.html.
[11] M. Farge, N. Kevlahan, V. Perrier, E. Goirand, Wavelets and turbulence, Proc. IEEE 84 (4) (1996) 639–669.
[12] J. Frohlich, K. Schneider, Computation of decaying turbulence in an adaptive wavelet basis, Physica D 134 (1999) 337–361.
[13] G. Garrigos, A. Tabacco, Wavelet decompositions of anisotropic Besov spaces, Math. Nachr. 239–240 (2002) 80–102.
[14] V. Girault, P.A. Raviart, Finite Element Methods for Navier–Stokes Equations, Springer-Verlag, Berlin, 1986.

[15] J.-P. Kahane, P.G. Lemarié-Rieusset, Fourier Series and Wavelets, Gordon & Breach, London, 1995.
[16] P.G. Lemarié-Rieusset, Analyses multi-résolutions non orthogonales, commutation entre projecteurs et dérivation et ondelettes vecteurs à divergence nulle, Rev. Mat. Iberoamericana 8 (2) (1992) 221–236 (in French).
[17] P.G. Lemarié-Rieusset, A. Jouini, Analyse multi-resolution bi-orthogonales sur l'intervalle et applications, Ann. IHP Sect. C 10 (4) (1993) 453–476.
[18] P.G. Lemarié-Rieusset, Un théorème d'inexistance pour les ondelettes vecteurs à divergence nulle, C. R. Acad. Sci. Paris Sér. I 319 (1994) 811–813 (in French).
[19] S. Mallat, A Wavelet Tour of Signal Processing, Academic Press, 1998.
[20] R. Masson, Biorthogonal spline wavelets on the interval for the resolution of boundary problems, Math. Models Methods Appl. Sci. 6 (1996) 749–791.
[21] S. Muller, Adaptive Multiscale Schemes for Conservation Laws, Lect. Notes Comput. Sci. Eng., vol. 27, Springer-Verlag, Berlin/Heidelberg, 2003.
[22] J.C. Nédélec, Acoustic and Electromagnic Equations Integral Representation for Harmonic Problems, Springer, New York, 2001.
[23] O. Pironneau, Méthodes d'éléments finis pour les fluides, Masson, 1988 (in French).
[24] D. Suter, Divergence-free wavelets made easy, in: A.F. Laine, M.A. Unser (Eds.), Wavelet Applications in Signal and Image Processing III, Proc. SPIE, vol. 2569, SPIE, Bellingham, 1995, pp. 102–113.
[25] K. Urban, Using divergence-free wavelets for the numerical solution of the Stokes problem, in: AMLI'96: Proceedings of the Conference on Algebraic Multilevel Iteration Methods with Applications, vol. 2, University of Nijmegen, The Netherlands, 1996, pp. 261–277.
[26] K. Urban, Wavelet bases in H(div) and H(curl), Math. Comp. 70 (234) (2000) 739–766.
[27] K. Urban, Wavelets in Numerical Simulation, Lect. Notes Comput. Sci. Eng., vol. 22, Springer-Verlag, 2002.